SAN098-2352J

Fluorinated Dodecaphenylporphyrins: Synthetic and Electrochemical Studies Including the First Evidence of Intramolecular Electron Transfer Between an Fe(II) Porphyrin •-Anion Radical and an Fe(I) Porphyrin

Karl M. Kadish,[1*] Eric Van Caemelbecke,[1] Francis D'Souza,[1] Min Lin,[1] Daniel J. Nurco,[2] Craig J. Medforth,[2*] Timothy P. Forsyth,[2] Bénédicte Krattinger,[2] Kevin M. Smith,[2] Shunichi Fukuzumi,[3] Ikuo Nakanishi,[3] John A. Shelnutt.[4]

[1]Department of Chemistry, University of Houston, Houston, TX 77204.

[2]Department of Chemistry, University of California, Davis, CA 95616.

[3]Department of Material and Life Science, Osaka University, Suita, Osaka 565-0871, Japan.

[4]Materials Theory and Computational Department, Sandia National Laboratories, Albuquerque, NM 87185-1349 and Department of Chemistry, University of New Mexico, Albuquerque, NM 87131.

For *Inorganic Chemistry.*

Sandia is a multiprogram laboratory operated by Sandia Corporation, a Lockheed Martin Company, for the United States Department of Energy under Contract DE-AC04-94AL85000.

DISCLAIMER

DISCLAIMER

Portions of this document may be illegible in electronic image products. Images are produced from the best available original document.

Synopsis

Dodecaphenylporphyrins with varying degrees of fluorination of the phenyl substituents (F_xDPPs) were synthesized as model compounds for investigating electronic effects in nonplanar porphyrins. Electrochemical studies of the chloroiron(III) complexes of these porphyrins revealed the expected anodic shifts upon fluorination, and also showed that the site of the second reduction was dependent on the substituents and the solvent (benzonitrile or pyridine). Evidence for an intramolecular electron transfer between an electrogenerated Fe(II) porphyrin •-anion radical and an Fe(I) porphyrin is presented.

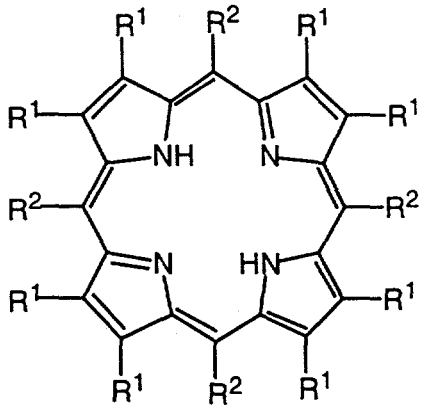

F_xDPPs

R^1 = phenyl or fluorophenyl

R^2 = phenyl or fluorophenyl

Abstract

Dodecaphenylporphyrins with varying degrees of fluorination of the peripheral phenyl rings (F_xDPPs) were synthesized as model compounds for studying electronic effects in nonplanar porphyrins, and detailed electrochemical studies of the chloroiron(III) complexes of these compounds were undertaken. The series of porphyrins, represented as FeDPPCl and as FeF_xDPPCl where x = 4, 8 (two isomers), 12, 20, 28 or 36, could be reversibly oxidized by two electrons in dichloromethane to give π-cation radicals and π-dications. All of the compounds investigated could also be reduced by three electrons in benzonitrile or pyridine. In benzonitrile, three reversible reductions were observed for the unfluorinated compound FeDPPCl, whereas the FeF_xDPPCl complexes generally exhibited irreversible first and second reductions which were coupled to chemical reactions. The chemical reaction associated with the first reduction involved a loss of the chloride ion after generation of $[Fe^{II}F_xDPPCl]^-$. The second chemical reaction involved a novel intramolecular electron transfer between the initially generated Fe(II) porphyrin π-anion radical and the final Fe(I) porphyrin reduction product. In pyridine, three reversible one electron reductions were observed with the second reduction affording stable Fe(II) porphyrin •- anion radicals for all of the complexes investigated.

Introduction

Recent studies of highly substituted porphyrins (e.g. **1-4** in Figure 1) have revealed many structural, spectroscopic and chemical changes associated with the substituent-induced nonplanarity present in such systems,[1-15] and have raised the question of whether nonplanar distortions may have a functional role in the energetics of biological systems.[16] The substituents in highly substituted porphyrins exert a complex mixture of steric effects (which dictate the amount and type of nonplanar distortion) and electronic effects (resulting from the electron-donating or electron-withdrawing abilities of the substituents) which can lead to some quite unexpected behavior. For example, progressive brominations of **5** (to ultimately yield **6**) initially produce the expected increase in half-wave potential for oxidation of the porphyrin, but then begin to decrease the oxidation potential as the degree of macrocyclic nonplanarity increases significantly for the more highly brominated analogs.[17-20] One aim of our research is to study the steric and electronic effects of substituents in nonplanar porphyrins and to obtain spectroscopic data which might be used to differentiate these effects in biologically important systems. To this end, we recently reported studies of a series of nickel(II) tetraalkylporphyrins **7 - 10** where the steric bulk of the peripheral substituents was used to vary the degree of porphyrin nonplanarity while the electronic properties of the substituents were held relatively constant.[21] In the work presented here, a series of porphyrins are described for which the converse should be true, namely that electronic effects of the peripheral substituents should predominate because the steric effects of the substituents are reasonably constant.

The series of porphyrins synthesized are based on the dodecaphenylporphyrin (DPP) framework (**4**) and have a total of 4, 8 (two isomers), 12, 20, 28 or 36 fluorines on the periperal phenyl rings (**11-17**). The fluorinated DPPs (F_xDPPs) were chosen for this work because they offered the greatest potential for varying electronic effects while at the same time minimizing differences in the steric effects of the substituents, and because existing synthetic methodology could be applied to the preparation of these materials. An investigation of the electrochemical properties of the chloroiron(III) complexes of DPP and the F_xDPPs (abbreviated as FeDPPCl and

$FeF_xDPPCls$) confirmed the dominance of electronic changes in the series; oxidation of the macrocycle (in CH_2Cl_2) became more difficult and reduction of the macrocycle or iron atom (in benzonitrile or pyridine) more facile as the degree of fluorination was increased. In addition, the electrochemical studies revealed that the site of the second reduction was strongly dependent on the macrocycle substituents and on the solvent. For the FeF_xDPPCl complexes in benzonitrile a novel intramolecular electron transfer between an initially generated Fe(II) porphyrin π-anion radical and a final Fe(I) porphyrin species was observed.

Materials and Methods

Spectroscopy.

^1H and ^{19}F NMR spectra were measured at frequencies of 300 MHz and 283 MHz, respectively. Spectra were typically recorded at ambient temperature (298 ± 5K) using 2 - 5 mM solutions in $CDCl_3$. ^1H chemical shifts were referenced to the chloroform solvent peak at δ 7.26. ^{19}F chemical shifts were referenced to CF_2Cl_2 at -8.0 ppm.[22] Visible absorption spectra were recorded on a Hewlett Packard 8450A spectrophotometer using CH_2Cl_2 as solvent. Mass spectra of the F_xDPPs were obtained using procedures described elsewhere.[23]

Electrochemistry.

Benzonitrile was distilled over P_2O_5 under vacuum, and pyridine was distilled over CaH_2 prior to use. Tetra-*n*-butylammonium perchlorate (TBAP) was recrystallized from ethyl alcohol and dried in a vacuum oven at 40 °C for at least one week prior to use. Cyclic voltammetry was carried out using an EG&G Model 173 potentiostat coupled with an EG&G Model 175 Universal Programmer or a BAS 100 Electrochemical Analyzer. Current-voltage curves were recorded on an EG&G Princeton Applied Research Model RE-0151 XY recorder. A three electrode system was used and consisted of a glassy carbon or platinum button working electrode, a platinum wire counter electrode, and a saturated calomel reference electrode (SCE). The reference electrode was separated from the bulk solution by a fritted-glass bridge filled with the solvent/supporting electrolyte mixture. Ferrocene was used as the internal standard, but all potentials are referenced

to the SCE. Solutions containing the metalloporphyrins were deoxygenated by a stream of nitrogen for at least 5 minutes prior to running the experiment and were also protected from air by a nitrogen blanket during the experiment. Thin-layer spectroelectrochemical measurements were carried out with a Tracor Northern 6500 multichannel analyzer/controller coupled with an EG&G model 173 Universal Programmer using an optically-transparent platinum thin-layer working electrode.[24] ESR spectra of the doubly reduced $FeF_{20}DPPCl$ generated electrochemically were taken on a JEOL JES-RE1XE by using an electrolysis cell designed for ESR measurements.[25] The controlled potential electrolysis of $FeF_{20}DPPCl$ was carried out in benzonitrile containing 0.2 M TBAP in the ESR cavity.

Syntheses of Pyrroles and Precursors.

3,4-Bis(4-fluorophenyl)pyrrole: The title compound was prepared by adapting a procedure used to prepare 3,4-diphenylpyrrole.[26] A 2 L 3-necked round bottomed flask was filled with anhydrous MeOH (1400 mL), NaOMe (211.7 g, 3.9 mol), and dimethyl N-acetyliminodiacetate (79.6 g, 0.39 mol) and brought to a gentle reflux under inert atmosphere. 4,4'-Difluorobenzil (96.4 g, 0.39 mol, Aldrich) was added and the solution was refluxed for an additional 25 minutes after which the reaction contents were poured into de-ionized H_2O (6 L). A precipitate formed and was filtered off and the aqueous filtrate was washed with diethyl ether (2 x 1 L). The residual diethyl ether and MeOH present in the aqueous solution were removed by partially stripping off the solvent *in vacuo*. The cooled concentrated aqueous solution was acidified with 6 M HCl resulting in the precipitation of a mix of diester and partially hydrolyzed diester diphenylpyrroles (34.2 g) which was filtered off.

To afford a complete saponification the crude diester diphenylpyrroles (32.3 g) were dissolved in 10% aqueous KOH (350 mL) and refluxed for 20 min. The stirred solution was chilled in an ice bath and neutralized by the addition of 6 M HCl which precipitated the diacid pyrroles. Filtration of the precipitate afforded a mixture of 3,4-bis(4-fluorophenyl)pyrrole-2,5-dicarboxylic acid, 3,4-bis(4-methoxyphenyl)pyrrole-2,5-dicarboxylic acid, and 3-(4-

fluorophenyl)-4-(4-methoxyphenyl)pyrrole-2,5-dicarboxylic acid as a brittle tan solid (32.1 g). The formation of methoxylated pyrroles presumably takes place via nucleophilic substitution of the aryl fluorines by methoxide.

The diacid diphenylpyrrole mixture (32.1 g) was dissolved in ethanolamine (200 mL) and refluxed for 2 h. The cooled reaction solution was poured into a mixture of H_2O (1 L) and saturated aqueous NaCl (500 mL) and the aqueous phase was extracted with CH_2Cl_2 (3 x 300 mL). The pooled organic extracts were dried over anhydrous Na_2SO_4 and stripped of solvent *in vacuo* to yield a dark brown residue. The residue was chromatographed on silica gel eluted with gradient mixtures of CH_2Cl_2/petroleum ether. After several columns and crystallizations from CH_2Cl_2/cyclohexane, three diphenylpyrroles were isolated in pure form. The least polar fractions afforded 3,4-bis(4-fluorophenyl)pyrrole (6.8 g, 0.027 mol, 6.9% yield based on starting 4,4'-difluorobenzil), while the most polar fractions afforded 3,4-bis(4-methoxyphenyl)pyrrole (4.5 g, 0.016 mol) in 4.1% yield. Of intermediate rf on silica gel was 3-(4-fluorophenyl)-4-(4-methoxyphenyl)pyrrole (3.5 g, 0.013 mol) which was isolated in 3.3% yield. Characterization data for these compounds are as follows:

3,4-Bis(4-fluorophenyl)pyrrole: ^{1}H NMR ($CDCl_3$), δ 8.29 (br s, 1H, NH), 7.19 (m, 4H, H_{ortho}) 6.95 (m, 4H, H_{meta}) 6.78 (d, J = 2.7 Hz, 2H, pyrrole-H_α). ^{13}C NMR ($CDCl_3$), δ 115.06 (d, J = 21.2 Hz, C_{meta}), 117.23 (s, C_α), 122.52 (s, C_β), 129.93 (d, J = 7.7 Hz, C_{ortho}), 131.50 (d, J = 2.7 Hz, C_{ipso}), 161.39 (d, J = 244.3 Hz, C_{para}). ^{19}F NMR ($CDCl_3$), δ -119.2 (m, F_{para}). Mp, 138-140° C. EI$^+$ HRMS: calcd 255.0860, found 255.0865 (M^+ 100). Anal. Calcd for $C_{16}H_{11}F_2N$: C 75.28, H 4.34, N 5.49; found: C 75.30, H 4.37, N 5.51. Alternate preparation - European Patent 0 334 147.

3,4-Bis(4-methoxyphenyl)pyrrole: ^{1}H NMR ($CDCl_3$), δ 8.20 (br s, 1H, NH), 7.18, 6.81 (d, 4H each, H_{ortho}, H_{meta}, J $H_{ortho}H_{meta}$ = 8.9 Hz), 6.79 (d, 2H, H_α), 3.76 (s, 6H, -OCH_3). ^{13}C NMR ($CDCl_3$), δ 55.14 (-OCH_3), 113.62 (C_{meta}), 116.75 (C_α), 122.96 (C_β), 128.42 (C_{ipso}), 129.53 (C_{ortho}), 157.76 (C_{para}). Mp 110.5 - 112.5° C. EI$^+$ HRMS: calcd 279.1259, found 279.1251 (M^+ 100). Anal. Calcd for $C_{18}H_{17}NO_2$: C 77.40, H 6.13, N 5.01; found: C 77.71, H 6.18, N 5.10.

3-(4-Fluorophenyl)-4-(4-methoxyphenyl)pyrrole: Isolated as an oil or glass like material. EI$^+$ HRMS: calcd 267.1059, found 267.1057 (M^+ 100).

3,4-Bis(3,5-difluorophenyl)pyrrole: 3,5,3',5'-Tetrafluorobenzil was prepared by adapting a standard procedure for the condensation of benzaldehyde into benzoin[27] followed by an oxidation to the corresponding benzil.[28] Thiamine hydrochloride (11.0 g, 0.033 mol) was dissolved in de-ionized H_2O (32 mL) followed by the addition of 95% ethanol (85 mL), 10% sodium hydroxide (32 mL), and 3,5-difluorobenzaldehyde (45.0 g, 0.317 mol, Indofine Chem. Co.). The mixture was stoppered, shaken vigorously, and allowed to sit for 3 days. The solution was then filtered and the filtrate washed with de-ionized H_2O and vacuum dried to afford 3,5,3',5'-tetrafluorobenzoin (36 g, 0.13 mol).

3,5,3',5'-Tetrafluorobenzoin (36 g, 0.13 mol) and aqueous acidic cupric acetate (16 mL 10% acetic acid containing 0.48 g cupric acetate dihydrate) were then dissolved in a solution of ammonium nitrate (12.7 g, 0.158 mol) in glacial acetic acid (80 mL). The reaction mixture was refluxed for 90 min, cooled, filtered, and the filtrate was washed with de-ionized H_2O. The crude product was recrystallized from MeOH to afford 3,5,3',5'-tetrafluorobenzil (28.0 g, 0.099 mol) in 62% yield (based on starting 3,5-difluorobenzaldehyde). ^{1}H NMR ($CDCl_3$), δ 7.5 (m, 4H, H_{ortho}), 7.1 (m, 2H, H_{para}). ^{19}F NMR ($CDCl_3$) δ: -108.0 (m, F_{meta}). Mp 135.0 - 136.5° C. EI$^+$ HRMS m/z for $C_{14}H_6F_4O_2$ M^+ (not found), however, a fragment (found: 141.0136) corresponds to $C_7H_3F_2O$ (calculated: 141.0151) which results from cleavage of the lone C-C single bond. Anal. Calcd for $C_{14}H_6F_4O_2$: C 59.59, H 2.14; found: C 59.66, H 2.11.

3,4-Bis(3,5-difluorophenyl)pyrrole was prepared by adapting a procedure used to prepare 3,4-diphenylpyrrole.[26] A 2 L 3-necked round bottomed flask was filled with anhydrous MeOH (600 mL), NaOMe (65.0 g, 1.20 mol), and dimethyl N-acetyliminodiacetate (110.4 g, 0.544 mol) and the solution was refluxed for 15 minutes under inert atmosphere. The reflux was temporarily stopped to allow the addition of 3,5,3',5'-tetrafluorobenzil (75.0 g, 0.266 mol) after which the solution was refluxed for an additional 40 minutes and poured into de-ionized H_2O (6 L). In some cases, a precipitate is observed when the reaction mixture is poured into de-ionized H_2O

and this was most evident when the reaction was carried out on a smaller scale. The precipitate was a reaction byproduct resulting from the benzil - benzilic acid rearrangement[29] of 3,5,3',5'-tetrafluorobenzil and was filtered off. The aqueous solution was washed with diethyl ether (2 x 2 L) and the residual diethyl ether and MeOH present in the aqueous solution were removed by partially stripping off the solvent *in vacuo*. The cooled concentrated aqueous solution was basified by the addition of NaOH (600 g) and boiled in two 4 L beakers for 30 minutes. The solutions were allowed to cool for 6 hours, placed in ice baths, and acidified by the dropwise addition of 6 M HCl to precipitate the diacid pyrrole. The precipitate was filtered off and dried *in vacuo* yielding 3,4-bis(3,5-difluorophenylpyrrole)-2,5-dicarboxylic acid as a tan solid (16.7 g, EI$^+$ HRMS: calcd 379.04677, found 379.04662).

3,4-Bis(3,5-difluorophenylpyrrole)-2,5-dicarboxylic acid (16.7 g) was dissolved in ethanolamine (250 mL) and refluxed for 2 h. The cooled solution was poured into a mixture of de-ionized H_2O (500 mL) and saturated aqueous NaCl (250 mL) and extracted with CH_2Cl_2 (3 x 150 mL). The combined organic extracts were washed with a mixture of de-ionized H_2O (500 mL) and saturated aqueous NaCl (250 mL), dried over anhydrous Na_2SO_4 and stripped of solvent *in vacuo* to afford a thick brown oil which solidified upon storage at -60° C and also remained a solid when warmed to room temperature. This material was chromatographed on a silica gel column eluted with CH_2Cl_2 to afford 3,4-bis(3,5-difluorophenyl)pyrrole (4.9 g, 0.017 mol) in 6.4% yield (based on 3,5,3',5'-tetrafluorobenzil). ^{1}H NMR ($CDCl_3$), δ 8.41 (br s, 1H, NH), 6.92 (d, 2H, J = 3.5 Hz, pyrrole-H_α), 6.75 (m, 4H, H_{ortho}), 6.66 (tt, 2H, H_{para}). ^{19}F NMR ($CDCl_3$), δ -112.3 (m, F_{meta}). Mp 185 °C. FAB HRMS [M]$^+$ calcd 291.0671, found 291.0675. Anal. Calcd for $C_{16}H_9F_4N$: C 65.98, H 3.11, N 4.81; found: C 65.75, H 3.03, N 4.78.

Syntheses of Porphyrins.

H_2DPP (4): H_2DPP was prepared as described previously.[30]

FeDPPCl: Iron was inserted into H_2DPP using a standard procedure.[31] H_2DPP (72 mg, 0.059 mmol) was dissolved in a mixture of pyridine (10 mL) and glacial acetic acid (10 mL) and the mixture was heated to 90° C under inert atmosphere. Saturated aqueous Fe_2SO_4 (4 mL) was

added and the solution was heated overnight at 100°C. The mixture was diluted with CH_2Cl_2 (100 mL) and the organic layer washed with 0.02 M HCl (2 x 250 mL). The organic layer was dried over anhydrous Na_2SO_4, filtered, and the solvent removed *in vacuo* to afford crude FeDPPCl. This material was chromatographed on a silica gel column using gradient mixtures of MeOH/CH_2Cl_2 (starting with neat CH_2Cl_2). The combined fractions were washed with 0.02 M HCl (250 mL), dried over anhydrous Na_2SO_4, filtered, and the solvent removed *in vacuo* thus affording FeDPPCl (48 mg, 0.037 mmol) in 62% yield. ^{1}H NMR ($CDCl_3$ plus KCN in CD_3OD), δ 9.55 (br, 8H) 7.69 (br, 16H), 7.23 (br t, 8H), 6.81 (br, 16H), 5.81 (br, 4H), 4.02 (br, 8H). FAB HRMS $[M-Cl]^+$ calcd 1276.4167, found 1276.4186. Visible (CH_2Cl_2), λ_{max} (nm, rel. int.): 454 (100), 536 (21.3), 576 (16.0).

H_2F_4DPPCl (11): The title compound was prepared by adapting a published procedure for the preparation of dodecaphenylporphyrins.[32,33] 4-Fluorobenzaldehyde (566 mg, 4.56 mmol) was dissolved in acetic acid (38 mL) and brought to reflux. Subsequently, 3,4-diphenylpyrrole (1.00 g, 4.56 mmol) dissolved in warm acetic acid (22 mL) was added to the refluxing solution. Reflux was continued for 14 h at which time DDQ (1.04 g, 4.56 mmol) was added to the reaction mixture and reflux was continued for another 60 minutes. The cooled reaction solution was poured into a mixture of de-ionized water (300 mL) and saturated aqueous NaCl (300 mL) and neutralized with aqueous NaOH. The aqueous layer was extracted with CH_2Cl_2 (3 x 200 mL), and the combined organic extracts washed with aqueous 5% NaOH, dried over anhydrous Na_2SO_4, and stripped of solvent *in vacuo*. The resulting material was chromatographed on a silica gel column using gradient mixtures of MeOH/CH_2Cl_2 (starting with neat CH_2Cl_2 and finishing with neat MeOH). The porphyrin-bearing fractions were crystallized from CH_2Cl_2/cyclohexane thus affording H_2F_4DPP (424 mg, 0.327 mmol) in 29% yield. ^{1}H NMR ($CDCl_3$), δ 7.47 (q, 8H, meso-H_{ortho}), 6.39 (t, 8H, meso-H_{meta}), 6.75 (m, 40H, β-phenyl protons). ^{19}F NMR ($CDCl_3$), δ -118.33 (m, meso-F_{para}). FAB HRMS $[MH]^+$ calcd 1295.4676, found 1295.4680. Visible (1% Et_3N in CH_2Cl_2) λ_{max} (nm), 464 (ε 182,000), 560 (8,000), 612 (7,200); (1% trifluoroacetic acid in CH_2Cl_2) λ_{max} (nm, rel. int.), 486 (100), 714 (20.9).

FeF_4DPPCl: Iron was inserted into H_2F_4DPP using a standard procedure.[31] $FeCl_2 \cdot (H_2O)_4$ (30 mg) was added to a refluxing solution of H_2F_4DPP (40 mg, 0.031 mmol) in DMF (6 mL). After 30 minutes the reaction mixture was allowed to cool to room temperature and 0.1N HCl was added. A precipitate appeared which was filtered off and washed with water. The precipitate was chromatographed on Grade III alumina with a 50:50 mixture of CH_2Cl_2/cyclohexane. The iron complex fraction was collected, washed with 0.1 M HCl and evaporated to dryness to afford a residue which was crystallized from CH_2Cl_2/n-hexane thus affording FeF_4DPPCl (18.5 mg, 0.013 mmol) in 43% yield. ^1H NMR ($CDCl_3$), δ 12.2 (br, 8H, meso-H_{meta}), 10.2 (br, 16H, β-H_{meta}), 8.2 (v br, 8H, meso-H_{ortho}), 7.1 (v br, 16H, β-H_{ortho}), 5.4 (v br, 8H, meso-H_{ortho}), 4.96 (s, 8H, β-H_{para}), 4.8 (v br, 16H, β-H_{ortho}). ^{19}F NMR ($CDCl_3$), δ -110.3 (m, β-F_{para}). FAB HRMS $[M\text{-}Cl]^+$ calcd 1348.3791, found 1348.3753. Visible (CH_2Cl_2) λ_{max} (nm), 450 (ε 90,300), 530 (17,600), 574 (13,000).

H_2F_8DPP (β) (12): Benzaldehyde (208 mg, 1.96 mmol) and 3,4-bis(4-fluorophenyl)pyrrole (500 mg, 1.96 mmol) were treated as described in the preparation of H_2F_4DPP to afford H_2F_8DPP (β) (435 mg, 0.318 mmol) in 65% yield. ^1H NMR ($CDCl_3$), δ 7.52 (d, 8H, meso-H_{ortho}), 6.95 (t, 4H, meso-H_{para}), 6.83 (t, 8H, meso-H_{meta}), 6.60 (m, 16H, β-H_{ortho}), 6.38 (t, 16H, β-H_{meta}). ^{19}F NMR ($CDCl_3$), δ -118.9. Mp > 300° C. MALDI FT-ICR MS $[MH]^+$ calcd 1367.4, found 1367.4. Visible (CH_2Cl_2) λ_{max} (nm), 464 (ε 170,000), 562 (11,000), 612 (10,600), 718 (5,200), (1% trifluoroacetic acid in CH_2Cl_2) λ_{max} (nm, rel. int.), 384 (19.7), 490 (100), 720 (23.2).

FeF_8DPPCl (β): Iron was inserted into H_2F_8DPP (β) (30 mg, 0.022 mmol) using the procedure described for $Fe^{III}F_4DPPCl$ and afforded $Fe^{III}F_8DPPCl$ (β) (15 mg, 0.010 mmol) in 45% yield. ^1H NMR ($CDCl_3$), δ 12.88 (br s, 8H, meso-H_{meta}), 9.51 (br s, 16H, β-H_{meta}), 8.1 (v br, 8H, meso-H_{ortho}), 6.8 (v br, 16H, β-H_{ortho}), 5.5 (v br, 8H, meso-H_{ortho}), 5.45 (br s, 4H, meso-H_{para}), 4.6 (v br, 16H, β-H_{ortho}). ^{19}F NMR ($CDCl_3$), δ -110.7 (β-F_{para}). FAB HRMS $[M\text{-}Cl]^+$ calcd 1420.3414, found 1420.3459. Visible (CH_2Cl_2) λ_{max} (nm), 450 (ε 85,200), 534 (17,000), 574 (12,600).

H_2F_8DPP (meso) (13): H_2F_8DPP(meso) was prepared by adapting a published procedure

for the preparation of dodecaphenylporphyrins.[32] A solution containing 3,4-diphenylpyrrole (0.90 g, 4.1 mmol) and 2,6-difluorobenzaldehyde (0.58 g, 4.1 mmol) in CH_2Cl_2 (500 mL) was purged with N_2 for 10 minutes after which $BF_3{\cdot}OEt_2$ (0.25 mL, 2 mmol) was added via syringe. The reaction mixture was shielded from the light and stirred for 24 h. After removal of the solvent *in vacuo* the solid obtained was refluxed for 2 h with DDQ (0.75 g, 3.3 mmol) in toluene (250 mL). The cooled solution was treated with triethylamine (0.5 mL) and the solvent was removed *in vacuo*. The resulting material was chromatographed on a silica gel column using gradient mixtures of MeOH/CH_2Cl_2 (starting with neat CH_2Cl_2). The porphyrin-bearing fractions were crystallized from CH_2Cl_2/cyclohexane thus affording H_2-*meso*-2,6-difluorophenyl-F_8DPP (1.1 g, 0.80 mmol) in 81% yield. ^{1}H NMR ($CDCl_3$), δ -1.09 (s, 2H, NH), 6.18 (dd, 8H, J_{HmHp} = 8.5 Hz, J_{HmF} = 7 Hz, meso-H_{meta}), 6.68 (t, 4H, J_{HpHm} = 8.5 Hz, meso-H_{para}), 6.73 - 6.78 (m, 24H, β-H_{para}, β-H_{meta}), 6.90 (m, 16H, β-H_{ortho}). ^{19}F NMR ($CDCl_3$), δ -108.55 (meso-F_{ortho}). LSIMS $[MH]^+$ calcd 1367.4, found 1368. Visible (CH_2Cl_2) λ_{max} (nm), 452 (ε 215,000), 546 (17,600), 624 (7,300), 689 (2,400).

FeF_8DPPCl (meso): Iron was inserted into H_2F_8DPP (meso) (48 mg, 0.035 mmol) using the procedure described for FeF_4DPPCl and afforded FeF_8DPPCl (meso) (30 mg, 0.021 mmol) in 60% yield. ^{1}H NMR ($CDCl_3$), δ 13.0 (br s, 4H, meso-H_{meta}), 12.6 (br s, 4H, meso-H_{meta}), 10.5 (br s, 8H, β-H_{meta}), 10.4 (br s, 8H, β-H_{meta}), 7.7 (v br, 8H, β-H_{ortho}), 6.4 (br s, 4H, meso-H_{para}), 5.1 (v br, 8H, β-H_{ortho}), 5.1(br s, 8H, β-H_{para}). ^{19}F NMR ($CDCl_3$), δ -80.3 (meso-F_{ortho}), -74.8 (meso-F_{ortho}). FAB HRMS $[M\text{-}Cl]^+$ calcd 1420.3414, found 1420.3361. Visible (CH_2Cl_2) λ_{max} (nm), 398 (ε 71,600), 436 (93,600).

H_2F_{12}DPP (14): 4-Fluorobenzaldehyde (486 mg, 3.92 mmol) and 3,4-bis(4-fluorophenyl)pyrrole (500 mg, 1.96 mmol) were treated as described in the preparation of H_2F_4DPP thus affording H_2F_{12}DPP (462 mg, 0.321 mmol) in 33% yield. ^{1}H NMR ($CDCl_3$), δ 7.47 (q, 8H, meso-H_{ortho}), 6.61 (m, 16H, β-H_{ortho}), 6.54 (t, 8H, meso-H_{meta}), 6.47 (t, 16H, β-H_{meta}). ^{19}F NMR ($CDCl_3$), δ -117.9 (β-F_{para}), 116.4 (meso-F_{para}). FAB HRMS $[MH]^+$ calcd 1439.3922, found 1439.3978. Visible (2% Et_3N in CH_2Cl_2) λ_{max} (nm), 462 (ε 182,000), 558 (11,100), 608 (10,000),

712 (5,000), (1% trifluoroacetic acid in CH_2Cl_2) λ_{max} (nm, rel. int.), 488 (100), 716 (27.4).

FeF_{12}DPPCl: Iron was inserted into H_2F_{12}DPP (40 mg, 0.028 mmol) using the procedure described for Fe F_4DPPCl and afforded FeF_{12}DPPCl (23 mg, 0.015 mmol) in 54% yield. ^{1}H NMR ($CDCl_3$), δ 12.5 (br, 8H, meso-H_{meta}), 9.7 (br, 16H, β-H_{meta}), 8.0 (v br, 4H, meso-H_{ortho}), 6.9 (v br, 8H, β-H_{ortho}), 5.4 (v br, 4H, meso-H_{ortho}), 4.5 (v br, 8H, β-H_{ortho}). ^{19}F NMR ($CDCl_3$), δ (ppm); -109.3 (β-F_{para}), -107.9 (meso-F_{para}). FAB HRMS $[M-Cl]^+$ calcd 1492.3037, found 1492.3072. Visible (CH_2Cl_2) λ_{max} (nm), 448 (ε 88,700), 534 (17,400), 576 (13,000).

H_2F_{20}DPP (15): Pentafluorobenzaldehyde (2.00 g, 10.2 mmol) and 3,4-diphenylpyrrole (2.24 g, 10.2 mmol) were treated as described in the preparation of H_2F_8DPP (meso) thus affording H_2F_{20}DPP (1.74 g, 1.1 mmol) in 44% yield. ^{1}H NMR ($CDCl_3$), δ 7.00 (br, 40H, β-H_{phenyl}). ^{19}F NMR ($CDCl_3$), δ -137.5 (d, 8F, F_{ortho}), -156.2 (t, 4F, F_{para}), -166.9 (t, 8F, F_{meta}). MALDI FT-ICR MS $[M+H]^+$ calcd 1583.3, found 1583.3. Visible (CH_2Cl_2) λ_{max} (nm), 444 (ε 164,000), 538 (10,200), 618 (1,970), (1% trifluoroacetic acid in CH_2Cl_2), λ_{max} (nm, rel. int.), 472 (100), 612 (6.54), 666 (5.12).

FeF_{20}DPPCl: Iron was inserted into H_2F_{20}DPP using a standard procedure.[34] Acetonitrile (50 mL) was refluxed for 30 minutes in oven dried glassware under an inert atmosphere. $FeCl_2 \cdot 4(H_2O)$ (899 mg, 4.52 mmol) was added to the refluxing mixture and subsequently H_2F_{20}DPP (143 mg, 0.090 mmol) dissolved in de-gassed $CHCl_3$ (12 mL) was added to the reaction mixture in a dropwise fashion. Stirring was continued for 10 minutes after complete addition of the porphyrinic solution. The reaction mixture was poured into CH_2Cl_2 (200 mL) and washed with 0.5 M HCl to convert the product to its FeCl form. The resulting material was chromatographed on a silica gel column using gradient mixtures of MeOH/CH_2Cl_2 (starting with neat CH_2Cl_2). Porphyrin-bearing fractions were washed with 0.5 M HCl, dried over anhydrous Na_2SO_4, and stripped of solvent *in vacuo* thus providing FeF_{20}DPPCl (122 mg, 0.073 mmol) in 81% yield. ^{1}H NMR ($CDCl_3$), δ 10.84 (br s, 16H, β-H_{meta}), 7.7 (v br, 8H, β-H_{ortho}), 5.3 (br s, 16H, β-H_{ortho}, β-H_{para}). ^{19}F NMR ($CDCl_3$), δ -98.1, -102.6 (br, 4F each, meso-F_{ortho}), -152.0 (br, 4F, meso-F_{para}), -156.0, -156.1 (br, 4F each, meso-F_{meta}). ^{1}H NMR ($CDCl_3$ + KCN in CD_3OD), δ 7.95

(d, 16H, β-H_{ortho}), 7.35 (t, 16H, β H_{meta}), 7.20 (t, 8H, β-H_{para}). ^{19}F NMR ($CDCl_3$ + KCN in CD_3OD), δ -160.3 (meso-F_{meta}), -156.3 (meso-F_{para}), -117.2 (meso-F_{ortho}). FAB HRMS $[M-Cl]^+$ calcd 1636.2283, found 1636.2275. Visible (CH_2Cl_2) λ_{max} (nm, rel. int.), 400 (76.7), 430 (100).

H_2F_{28}DPP (16): 3,4-Bis(4-fluorophenyl)pyrrole (500 mg, 2.0 mmol) and pentafluorobenzaldehyde (0.24 ml, 2.0 mmol) were treated as described in the preparation of H_2F_8DPP (meso) and afforded H_2F_{28}DPP (150 mg, 0.087 mmol) in 17% yield. ^{1}H NMR ($CDCl_3$), δ -1.51 (br s, 2H, NH), 6.73 (t, 16H, β-H_{meta}), 6.94 (m, 16H, β-H_{ortho}). ^{19}F NMR ($CDCl_3$), δ -136.14 (meso-F_{ortho}), -153.02 (meso-F_{para}), -164.42 (meso-F_{meta}), -113.68 (β-F_{para}). MALDI FT-ICR MS $[M+H]^+$ calcd 1727.2, found 1727.2. Visible (CH_2Cl_2) λ_{max} (nm), 442 (ε 174,000), 538 (17,200), 616 (7,100), (1% trifluoroacetic acid in CH_2Cl_2) λ_{max} (nm, rel. int.), 490 (100), 630 (10.4), 692 (9.7).

FeF_{28}DPPCl: Iron was inserted into H_2F_{28}DPP (52.2 mg, 0.031 mmol) using the procedure described for FeF_{20}DPP Cl and afforded FeF_{28}DPPCl (41 mg, 0.023 mmol) in 75% yield. ^{1}H NMR ($CDCl_3$), δ 10.3 (br s, 8H, β-H_{meta}), 10.2 (br s, 8H, β-H_{meta}), 7.7 (very br s, 8H, β-H_{ortho}), 5.2 (very br s, 8H, β-H_{ortho}). ^{19}F NMR ($CDCl_3$), δ -155.4 (meso-F_{meta}), -155.1 (meso-F_{meta}), -149.9 (meso-F_{para}), -106.4 (β-F_{para}), -103.1 (meso-F_{ortho}), -97.9 (meso-F_{ortho}). ^{1}H NMR ($CDCl_3$ + KCN in CD_3OD), δ 8.12 (m, 16H, β-H_{ortho}), 7.16 (t, 16H, β-H_{meta}). ^{19}F NMR ($CDCl_3$ + KCN in CD_3OD), δ -160.0 (meso-F_{meta}), -155.3 (meso-F_{para}), -117.3 (meso-F_{ortho}), -116.3 (β F_{para}). FAB HRMS $[M-Cl]^+$ calcd 1780.1529, found 1780.1488. Visible (CH_2Cl_2) λ_{max} (nm), 387 (ε 61,400), 430 (94,000).

H_2F_{36}DPP (17): 3,4-Bis(3,5-difluorophenyl)pyrrole (1.00 g, 3.43 mmol) and pentafluorobenzaldehyde (0.673 g, 3.43 mmol) were treated as described in the preparation of H_2-*meso*-2,6-difluorophenyl-F_8DPP. Silica gel column chromatography ($CHCl_3$ eluent) afforded the desired product along with a red contaminant which runs at the same rf on silica gel and cannot be removed in this fashion. The red contaminant was removed by crystallization from CH_2Cl_2/cyclohexane thus affording pure crystalline H_2F_{36}DPP (175 mg, 0.094 mmol) in 10.9% yield. ^{1}H NMR (acetone-d_6), δ 7.01 (m, 24H). ^{19}F NMR (acetone-d_6), δ -165.7 (meso-F_{meta}), -

154.2 (meso-F_{para}), -135.3 (meso-F_{ortho}), -111.4 (β-F_{meta}). FAB HRMS $[M]^+$ calcd 1870.1583, found 1870.1629. Visible (CH_2Cl_2) λ_{max} (nm), 444 (ε 179,000), 540 (15,000), 572 (6,690), 620 (5,450), (1 % trifluoroacetic acid in CH_2Cl_2) λ_{max} (nm, rel. int.), 480 (100), 616 (6.9), 676 (7.2).

FeF_{36}DPPCl: Iron was inserted into H_2F_{36}DPP (35 mg, 0.019 mmol) using the procedure described for FeF_{20}DPPCl and afforded FeF_{36}DPPCl (29 mg, 0.015 mmol) in 78% yield. ^1H NMR ($CDCl_3$), δ 6.5 (br, 16H, β-H_{ortho}), 4.9 (br, 8H, β-H_{para}). ^{19}F NMR ($CDCl_3$), δ -97.1, -103.6 (br, 4F each, meso-F_{ortho}), -107.0, -108.3 (br, 8F each, β-F_{meta}), -147.5 (br, 4F, meso-F_{para}), -153.5, -154.2 (br, 4F each, meso-F_{meta}). FAB HRMS $[M-Cl]^+$ calcd 1924.078, found 1924.060. Visible (CH_2Cl_2) λ_{max} (nm, rel. int), 391 (65.6), 430 (100), 560 (15.6).

Results and Discussion

Synthetic Studies

The series of F_xDPPs presented in this paper are the most recent additions to a growing collection of porphyrins based on the DPP framework.[33,35] At present, it appears that the preparation of F_xDPPs with even more electron-withdrawing fluorophenyl groups is not feasible. For example, we attempted to prepare 3,4-bis-(2,6-difluorophenyl)pyrrole in the hope that it could be reacted with pentafluorobenzaldehyde to afford the more electron-withdrawing H_2F_{36}DPP isomer **18**. However, when 2,6,2',6'-tetrafluorobenzil was used in the same base-catalyzed reaction employed to make 3,4-bis-(3,5-difluorophenyl)pyrrole, the only product isolated was methyl 2,6,2',6'-tetrafluorobenziloate (some methyl benziloate was obtained in the synthesis of 3,4-bis-(4-fluorophenyl)pyrrole, and the methyl benziloate was the major product obtained from the synthesis of 3,4-bis-(3,5-difluorophenyl)-pyrrole). The fact that the methyl benziloate becomes the major product as the fluorination of the benzil is increased is consistent with a report in the literature that fluorination increases the rate of the benzilic acid rearrangement.[36] A second route involving a base catalysed condensation was also used in an attempt to prepare 3,4-bis-(2,3,4,5,6-pentafluorophenyl)pyrrole, which upon reaction with pentafluorobenzaldehyde might yield the perfluorododecaphenylporphyrin H_2F_{60}DPP (**19**).

However, reaction of 1-cyano-1,2-bis(2,3,4,5,6-pentafluorophenyl)ethene with ethyl isocyanoacetate[37] yielded 2,4-dicarbethoxy-3-(2,3,4,5,6-pentafluorophenyl)pyrrole as the principle product; a similar product has been reported during the preparation of 3,4-dialkylpyrroles using the same reaction.[38]

Given the difficulties encountered in preparing 3,4-diphenylpyrroles with highly fluorinated phenyl rings, as well as the problems inherent in condensing electron deficient pyrroles with aldehydes,[39] we turned our attention to the recently reported Suzuki coupling reaction of aryl boronic acids with **3** to give dodecaarylporphyrins.[40] The Suzuki coupling reactions worked well with phenylboronic acid, 4-chlorophenylboronic acid, and 3,5-dichlorophenylboronic acid.[41] However, the reactions of 2,6-difluorophenylboronic acid or 2,3,4,5,6-pentafluorophenylboronic acid with **3** did not give the expected products $H_2F_{16}DPP$ (**20**) or $H_2F_{40}DPP$ (**21**). Further investigations of the uses of the Suzuki coupling reaction to prepare novel DPPs will be reported shortly.[41]

Electrochemical Studies

The electrochemistry of iron porphyrins has been carried out in a variety of non-aqueous solvents.[42,43] Low valent iron porphyrins are known to react with chlorinated hydrocarbons such as CH_2Cl_2 to give sigma bonded Fe(III) derivatives,[44] so we used CH_2Cl_2 as a solvent only for oxidation reactions. Benzonitrile or pyridine were employed for the reduction reactions.

Electrooxidation in CH_2Cl_2. Cyclic voltammograms for the oxidation of representative FeF_xDPPCl derivatives in CH_2Cl_2 with 0.1M TBAP are shown in Figure 2, while Table 1 summarizes the half-wave potentials of each investigated complex along with those for the well-studied FeTPPCl and FeOEPCl under the same experimental conditions. The F_xDPP derivatives with x = 0 - 20 undergo two well-defined one-electron transfer processes while $FeF_{28}DPPCl$ and $FeF_{36}DPPCl$ show only a single oxidation within the anodic potential range of the solvent. The redox reactions are straightforward and the overall reactions proceed as shown in Scheme I, where P represents F_xDPP and the final products are formulated as Fe(III) porphyrin •-radical cations and π-dications, respectively.[42,43]

Scheme I

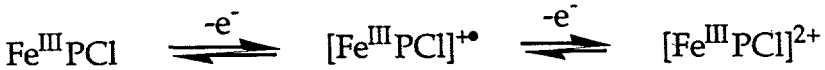

As was earlier reported,[45] FeDPPCl is much easier to oxidize ($E_{1/2}$ = 0.73 V) than either FeTPPCl ($E_{1/2}$ = 1.14 V) or FeOEPCl ($E_{1/2}$ = 1.08 V), something which would not be expected based on the electronic effects of the substituents. The easier oxidation of FeDPPCl is consistent with the fact that the compound adopts a very nonplanar conformation in solution.[1,3,46]

The oxidation potentials of the FeF_xDPPCls show the expected increase with the degree of fluorination of the peripheral phenyl rings, with $\Delta_{FLUORINATION}$ for the first oxidation potential changing by approximately 720 mV within the series (Table 1). The electron withdrawing ability of the fluoro groups is strongly dependent on their position on the peripheral phenyl rings, with para fluoro groups in FeF_8DPPCl (β) causing only a small increase in the oxidation potential whereas the ortho fluoro groups in FeF_8DPPCl (meso) causing a much larger effect. Attempts were made to correlate the oxidation potentials seen for the FeF_xDPPCl complexes with empirical measures of the electron-withdrawing ability of the substituents (Hammett σ values) in the hope that this would reveal any changes in the oxidation potential resulting from nonplanarity rather than electronic effects. However, because of differences in the reported Hammett σ values for fluorophenyl substituents, and the fact that substituent parameters were not available for some substituents, it was not possible to use this procedure to determine if the oxidation potentials contained a steric (nonplanarity) component. A more detailed investigation of the substituent effects in these and other F_xDPP complexes is in progress and will be reported shortly.[47]

Finally, a comparison of the oxidation potentials for FeDPPCl and $FeF_{20}DPPCl$ shows that the potential difference is somewhat greater for the first oxidation (630 mV) than for the second oxidation (450 mV). Indeed, the second oxidation of the FeF_xDPPCls is virtually unaffected by the addition of 4, 8 or 12 F groups at the *para* position of the phenyl rings in DPP,

F_4DPP, F_8DPP or F_{12}DPP. This lack of a substituent effect of the F groups on the second oxidation is reflected in the absolute potential separation between the two redox processes of a given compound (Δox) which systematically decreases from 0.46 V for FeDPPCl to 0.34 V for FeF_{12}DPPCl (Table 1).

Electroreduction in Benzonitrile. Figure 3 shows the reduction of four representative FeF_xDPPCl derivatives (x = 0, 20, 28 and 36) in benzonitrile containing 0.1 M TBAP. Two types of behavior are observed. The first is for FeDPPCl which undergoes three reversible one-electron reductions at $E_{1/2}$ = -0.36, -0.99 and -1.76 V. A different type of behavior is seen for the FeF_xDPPCl derivatives whose first two reductions are generally coupled with chemical reactions and show large separations between the cathodic and anodic peak potentials (see Table 2 and Figure 3). The separations between the anodic and cathodic peak potentials, $|E_{pa} - E_{pc}|$, are equal to 0.68 and 0.51 V for the first reduction of the F_{20} and F_{28} derivatives and 0.73 V for the first reduction of FeF_{36}DPPCl.

The irreversible nature of the Fe(III)/Fe(II) process for the FeF_xDPPCl complexes is characterized by current-voltage curves similar to those reported for FeTPPCl or FeOEPCl under several experimental conditions.[42,43] The prevailing mechanism for these reductions is shown in Scheme II, where processes I' and I correspond to the reduction and reoxidation peaks of the Fe(III)/Fe(II) process as indicated in Figure 3.

Scheme II

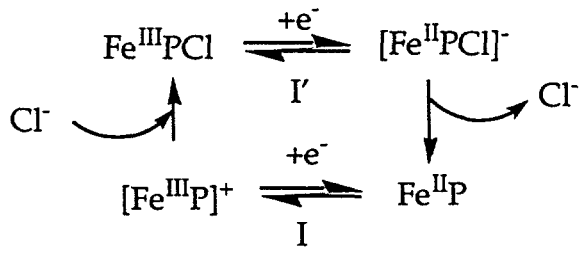

The formation of a spectrally detectable Fe(II) porphyrin product containing bound Cl^-

after reduction of FeTPPCl, i.e. $[Fe^{II}TPPCl]^-$, has been documented in the literature.[48] The mechanism in Scheme II was confirmed by the addition of excess TBACl to solutions of the FeF_xDPPCl complexes, which resulted in a complete reversibility for the first reduction as shown in Figure 4 for the case of $FeF_{20}DPPCl$.

The electrochemical data in Table 2 and Figure 3 might at first suggest a similar "box mechanism" involving the slow loss of Cl^- upon the conversion of $[FeF_xDPPCl]^-$ to its doubly reduced form (reaction II'). However, based upon electrochemical and spectroscopic data the "box mechanism" was rejected in favor of the one where forms A and B are assigned as an Fe(II) porphyrin •-anion radical and an Fe(I) porphyrin, respectively (Scheme III). In this case, the second electron transfer for the fluorinated compounds occurs at the macrocycle (process II') and is followed by an intramolecular electron transfer to give the iron(I) porphyrin species. The latter is reoxidized via process II to give $Fe^{II}P$.

Scheme III

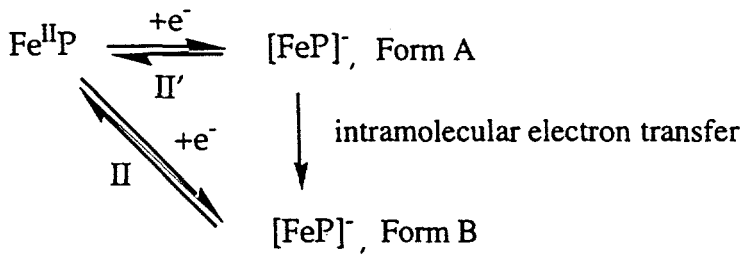

Our assignment of Form A as an Fe(II) porphyrin •-anion radical for the FeF_xDPPCl compounds is consistent with the much more difficult reduction versus reoxidation (e.g., E_{pc} = -1.31 V and E_{pa} = -0.90 V for F_4DPP) and the fact that the second reductions of the F_4DPP, F_8DPP and $F_{12}DPP$ derivatives occur at potentials similar to the first macrocycle-centered reduction of MDPP where M = Zn (-1.34 V), Cu (-1.32 V), or Pd (-1.32 V).[45] In addition, the reoxidation peak after the chemical reaction involving doubly reduced FeF_xDPPCl occurs at potentials more positive than those for the metal-centered Fe(I)/Fe(II) reaction of FeDPPCl,

consistent with a metal-centered reoxidation whose $E_{1/2}$ has been shifted by the electron-withdrawing F groups.

UV-visible spectroelectrochemical data were obtained for $FeF_{20}DPPCl$ and are consistent with the electrochemical results. The spectral changes upon the first reduction of $FeF_{20}DPPCl$ in benzonitrile are illustrated in Figure 5a and a summary of the spectral data is given in Table 3. The spectral changes during reduction are similar to those reported for other iron(III) porphyrins bearing an anionic axial ligand[19,49] and the data in Figure 5a are consistent with the generation of either $[Fe^{II}F_{20}DPPCl]^-$ or $Fe^{II}F_{20}DPP$ as a final reduction product after addition of one electron. The current-voltage curves for this electrode reaction are consistent with an EC mechanism where the chemical step, C, involves Cl^- dissociation. Thus, $Fe^{II}F_{20}DPP$ is the expected final porphyrin product after complete electrolysis of $Fe^{III}F_{20}DPPCl$ at -0.5 V. The spectral changes after reduction of $FeF_{20}DPPCl$ by one electron are reversible and the UV-visible spectrum of the initial Fe(III) porphyrin could be regenerated by controlled-potential oxidation at 0.8 V. This spectrum could also be recovered by switching the potential back to 0.8 V after the *second* one-electron reduction of $FeF_{20}DPPCl$.

The UV-visible data does not unambiguously distinguish between electrogeneration of an Fe(II) porphyrin π anion radical or an Fe(I) porphyrin in the second one-electron addition. However, because the second reduction is irreversible by cyclic voltammetry at a scan rate of 0.1V/s in benzonitrile (see Figure 3), the porphyrin product detected in solution by thin-layer UV-visible spectroelectrochemistry should be Form B (i.e. $[Fe^{I}F_{20}DPP]^-$) on the slower spectroelectrochemistry timescale. Iron(I) porphyrins have been reported to have a split Soret band and broad absorption bands between 700 and 800 nm,[50] and both of these Fe(I) features are present in the UV-visible spectrum generated after complete electrolysis of $Fe^{II}F_{20}DPP$ at -1.4 V.

The initial generation of an Fe(II) porphyrin π-anion radical and the subsequent conversion to an Fe(I) porphyrin as a final product of the two-electron reduction is further confirmed by the ESR spectrum for doubly reduced $FeF_{20}DPPCl$ in benzonitrile (Figure 6a).

When the doubly reduced $FeF_{20}DPPCl$ was generated chemically by the reduction of $FeF_{20}DPPCl$ (1.0 mM) with two equivalents of $Ru(bpy)_3^+$ (2.0 mM) in benzonitrile, the ESR spectrum taken just after the reduction at 77 K in Figure 6a shows both an isotropic signal (g = 2.003) and an anisotropic signals characteristic of an axially symmetric spin system ($g_{//}$ = 1.955 and $g_{\perp}$ = 2.168). The isotropic signal can be assigned to an Fe(II) porphyrin π-anion radical, while the anisotropic signal is similar to that of $[Fe^{I}TPP]^-$ ($g_{//}$ = 1.93 and $g_{\perp}$ = 2.28)[51] and $[Fe^{I}TPPBr_7]^-$, ($g_{//}$ = 1.96 and $g_{\perp}$ = 2.21).[50] When the doubly reduced $FeF_{20}DPPCl$ was generated electrochemically, the anisotropic signal was mainly observed with a trace amount of the isotropic signal. Thus, the two-electron reduction of $FeF_{20}DPPCl$ results in the initial formation of the Fe(II) porphyrin π-anion radical which is then converted to the Fe(I) porphyrin via intramolecular electron transfer. The two-electron reduction of $FeF_{28}DPPCl$ (1.0 mM) with two equivalents of $Ru(bpy)_3^+$ (2.0 mM) also results in formation of both the Fe(II) porphyrin π-anion radical (g = 2.004) and the Fe(I) porphyrin ($g_{//}$ = 1.954 and $g_{\perp}$ = 2.158).

The reduction site for Fe(II) porphyrins had been a major point of controversy in the literature for a number of years prior to the definitive ESR study by Bocian and co-workers[50] which showed that an iron(II) porphyrin π-anion radical or an iron(I) porphyrin could be observed depending upon the substituents on the macrocycle. Porphyrins with the most electron-withdrawing substituents favored reduction at the macrocycle, as the porphyrin e_g orbitals were at lower energy than the metal $d_{x^2-y^2}$ and d_{z^2} orbitals. Alternatively, porphyrins with the least electron-withdrawing substituents underwent reduction at the iron center because the d_{z^2} orbitals were lower in energy than the porphyrin e_g orbitals. A similar explanation can be offered for the DPP and F_xDPP complexes investigated in this study, where reduction of the electron-deficient FeF_xDPPCls also takes place at the macrocycle. More sigificantly, the FeF_xDPPCl complexes clearly demonstrate the conversion of an Fe(II) porphyrin •-anion radical to an Fe(I) porphyrin via intramolecular electon transfer.

The third reduction of FeF_xDPPCl is spectrally and electrochemically reversible in benzonitrile (see Figures 3 and 5) and is proposed to involve a conversion of the Fe(I) porphyrin

to an Fe(I) • anion radical, thus giving the electron transfer processes shown in Scheme IV for the overall three-electron reduction of the compounds investigated. Each FeF_xDPPCl derivative has a potential separation of 740-820 mV between $E_{1/2}$ of process III and E_{pa} of process II, which is similar to the 770 mV separation between processes III and II of FeDPPCl where the second reduction involves formation of Fe(I) followed by formation of an Fe(I) • anion radical at more negative potentials.

Scheme IV

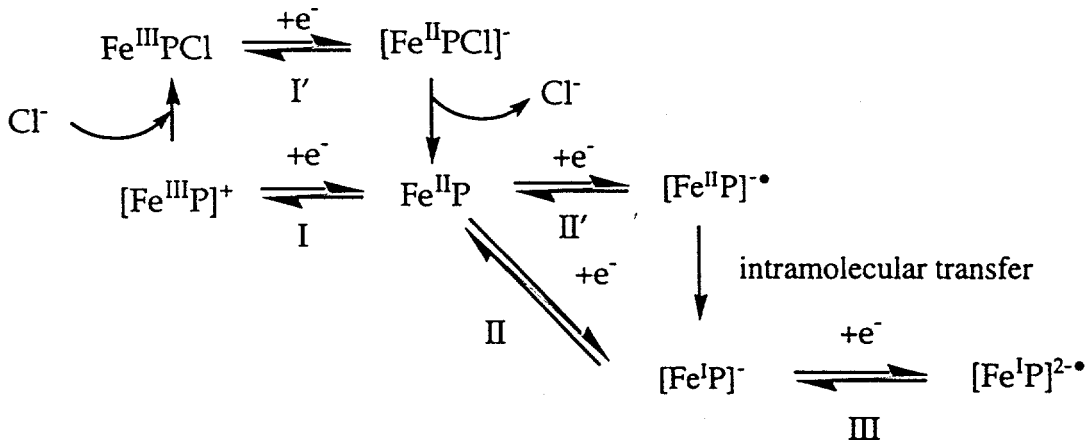

The reduction potentials of the FeF_xDPPCl complexes in benzonitrile (Table 2) clearly show the same anodic shifts seen when the compounds were oxidized in CH_2Cl_2 (Table 1). The range of potentials ($\Delta_{FLUORINATION}$) seen for the metal-centered reduction process I' [$Fe^{III}PCl$ -> $Fe^{II}PCl]^-$ was 450 mV, versus 430 mV for the macrocycle-centered second reduction process II' [$Fe^{II}P$ -> $Fe^{II}P^-$] and 660 mV for the macrocycle-centered third reduction process III [$Fe^{I}P$ -> $Fe^{I}P^-$]. $\Delta_{FLUORINATION}$ values for the corresponding reoxidations were larger, with process I giving $\Delta_{FLUORINATION}$ = 860 mV and process II showing $\Delta_{FLUORINATION}$ = 690 mV. These can be compared to a $\Delta_{FLUORINATION}$ value of 720 mV for the first macrocycle-centered oxidation process.

Electroreduction in Pyridine. Figure 7 illustrates cyclic voltammograms for reduction of four of the FeF_xDPPCl derivatives in pyridine with 0.1 M TBAP. The potentials for each

redox process are summarized in Table 4 which also includes data for FeOEPCl and FeTPPCl. Each FeF_XDPPCl complex undergoes three one-electron transfers which are labeled as processes I to III. The reversible half wave potentials shift anodically in potential with increased degree of fluorination. A 340-570 mV anodic shift in the Fe(III)/Fe(II) process is also observed for each given compound upon going from benzonitrile to pyridine as a solvent and this can be interpreted in terms of $[FeF_XDPP(py)_2]^+$ formation in the coordinating pyridine solvent. A similar assignment has been made in the case of FeTPPCl.[43,48]

Figure 5 illustrates the UV-visible spectroelectrochemical results for the first, second, and third one-electron reductions of $FeF_{20}DPPCl$ in pyridine. A summary of the spectral data in Figure 5 is also given in Table 3. The wavelengths of maximum absorbance in pyridine differ significantly from values in benzonitrile, as seen in Figure 5 for the case of $FeF_{20}DPPCl$. The spectrum of the neutral compound in pyridine has a single Soret band at 441 nm and a broad visible band at 586 nm. In contrast, the spectrum in benzonitrile has a Soret band at 432 nm, a shoulder at 389 nm and no well-defined visible bands between 500 and 800 nm. The singly reduced product of $[Fe^{III}F_{20}DPP(py)_2]^+$ complex has a 588 nm band in pyridine and this suggests that the initial porphyrin may actually exist as a mixture of Fe(II) and Fe(III) forms of the porphyrin in pyridine, which is perhaps not unexpected given the extremely positive Fe(III)/Fe(II) reduction potential of 0.45 V.

The spectral changes upon controlled potential reduction of $FeF_{20}DPPCl$ at 0.2 V in pyridine are similar to those after reduction in benzonitrile (see Figure 5) and indicate that a pure iron(II) form of the compound is electrogenerated in both cases. The spectral changes are reversible and the UV-vis spectrum of $[Fe^{III}F_{20}DPP(py)_2]^+$ could be fully regenerated upon controlled-potential oxidation at 0.6 V. The iron(II) porphyrin electrogenerated in pyridine has a UV-visible spectrum which differs from that of the electrogenerated iron(II) complex in benzonitrile, consistent with the known pyridine binding to Fe(II) porphyrins.[43,48]

The Soret and visible bands collapse during the second one-electron reduction of $FeF_{20}DPPCl$, while the band at 351 nm blue shifts to 323 nm and two new bands emerge at 609

and 794 nm. The data in Figure 5 resemble those obtained during the second reduction of the same compound in benzonitrile. However, closer examination of the data in Table 3 suggests that the doubly reduced product in the two solvents has a different formulation. This would be consistent with the different electrochemical behavior of the FeFxDPPCl complexes in benzonitrile and pyridine i.e. the second reduction is reversible in pyridine by both regular and thin-layer cyclic voltammetry. The doubly reduced product in pyridine is proposed to exist as the Fe(II) porphyrin •-anion radical $[Fe^{II}F_{20}DPP(py)_x]^{-\bullet}$ where x = 1 or 2. This is confirmed by the ESR spectrum of doubly reduced $FeF_{20}DPPCl$ (1.0 mM) produced by the reduction with two equivalents of $Ru(bpy)_3^+$ (2.0 mM) in pyridine (Figure 6b). In this case, only an isotropic ESR signal due to an Fe(II) porphyrin • anion radical (g = 2.003) is observed. No anisotropic signal due to an Fe(I) porphyrin are seen in pyridine, in contrast to the results obtained in benzonitrile (Figure 6a). A similar isotropic signal (g = 2.004) was observed for doubly reduced $FeF_{28}DPPCl$ in pyridine.

$[Fe^{II}F_{20}DPP(py)_x]^{-\bullet}$ is further reduced to an Fe(I) π -anion radical as shown by the fact that the UV-visible spectra of triply reduced $FeF_{20}DPPCl$ are virtually the same in benzonitrile and pyridine (see Figure 5c). The overall electroreduction mechanism in pyridine for each investigated FeF_xDPPCl complex is thus that shown in Scheme V.

Scheme V

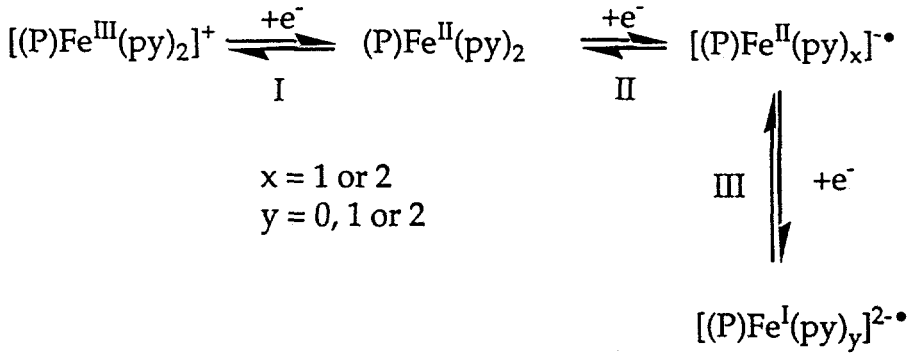

The tendency for the FeF_xDPPCls in pyridine to be reduced at the macrocycle but not to undergo electron transfer to the metal site can be interpreted in terms of exial ligation raising the energy of the d_{z2} orbital and effectively destabilizing the iron(I) porphyrin compared to the iron(II) porphyrin π-anion radical.[50] Finally, it should be noted that the large anodic shifts ($\Delta_{FLUORINATION}$ values) previously seen in the FeF_xDPPCl series for oxidation in CH_2Cl_2 (Table 1) or reduction in benzonitrile (Table 2) are also seen for reduction in pyridine (Table 4). The fluorination shifts range from +580 to +700 mV for the three processes observed.

Electroreduction of DPP and FxDPP Complexes With Other Metals: The electrochemical data obtained for DPP and $MF_{20}DPP$ complexes with other metals (Table 5 and Figure 8) fully support the earlier suggestion that the FeDPPCl and FeFxDPPCl complexes are reduced at the metal and at the macrocycle, respectively, in benzonitrile. The macrocycle-centered reductions of CuDPP, NiDPP, and ZnDPP are located at potentials of -1.22 to -1.34 V. In contrast, the potential for the reduction of FeDPPCl in benzonitrile ($E_{1/2}$ = -0.99 V) is lower and is similar to that seen for the first metal-centered reduction of CoDPP ($E_{1/2}$ = -0.97 V in CH_2Cl_2).[45] As expected, the Fe(II) complex also shows a larger absolute potential difference between the two reductions (Δ = 0.77 V) compared to the Zn(II), Cu(II) and Ni(II) DPP complexes (Δ = 0.39-0.49 V). These results are in contrast to those obtained for the corresponding $F_{20}DPP$ derivatives (Table 5 and Figure 8) where the reduction potential of the FeDPP complex (E_{pc} = -1.14 V) is similar to those seen for the macrocycle-centered reductions of ZnDPP and NiDPP ($E_{1/2}$ = -1.04 and -0.96 V). Note that the anodic peak potential for reoxidation of $[FeF_{20}DPP]^-$ in benzonitrile is located at a potential almost 500 mV more *positive* than E_{pa} for reoxidation of the other $[MF_{20}DPP]^-$ derivatives, which is consistent with the metal-centered nature of the reoxidation reaction for this species.

Conclusions

We have synthesized the dodecaphenylporphyrins **4** (DPP) and **11-17** (F_xDPPs) with the aim of preparing a series of very nonplanar porphyrins with different electronic properties but

similar steric (nonplanarity) effects. Electrochemical investigations of the chloroiron(III) complexes of these porphyrins (abbreviated as FeDPPCl and FeFxDPPCls) revealed the anodic shifts expected upon fluorination, with the first oxidation potential (FePCl -> $[FePCl]^{+\bullet}$) increasing by +720 mV between FeDPPCl and $FeF_{28}DPPCl$ in CH_2Cl_2/0.1 M TBAP. The porphyrin macrocycle and iron atom also become easier to reduce upon fluorination (e.g. $[Fe^{II}P]$ -> $[Fe^{II}P]^-$ = +700 mV for FeDPPCl and $FeF_{36}DPPCl$ in pyridine). In addition, the electrochemical studies show that the site of reduction for the iron complexes depends upon the solvent and whether the macrocycle is fluorinated. The site of reduction in iron(II) porphyrins had been an area of controversy in the field of porphyrin electrochemistry prior to the definitive ESR studies by Bocian and co-workers,[50] which indicated that the iron(II) porphyrin π-anion radicals or iron(I) porphyrins could be obtained depending upon the electron-withdrawing abilities of the substituents. The electrochemical and ESR data presented here show that reduction of (nonfluorinated) $Fe^{II}DPP$ in benzonitrile yields an iron(I) porphyrin whereas reduction of the FeF_xDPP complexes in benzonitrile produces an iron(II) porphyrin π-anion radical. Unusually, in the case of the FeF_xDPP complexes, the conversion of the initially produced iron(II) porphyrin π-anion radical to a final iron(I) porphyrin species can also be observed. In contrast to the behavior seen in benzonitrile, all of the complexes yield iron(II) porphyrin π-anion radicals when electroreduced in pyridine.

Additional studies of the FxDPPs described here are currently in progress. These include attempts to correlate the oxidation and reduction potentials of the F_xDPPs with empirical measures of the electron-donating or electron-withdrawing abilities of the substituents, spectroscopic parameters such as the positions of optical absorption and resonance Raman bands, and the catalytic oxygenation activity in the case of the iron complexes. We are also trying to determine how the effects of electron-withdrawing groups in very nonplanar porphyrins differ from those in nominally planar porphyrins, and to what extent fluorination might change the structures of the F_xDPPs. On the latter point, it should be noted that since we began this project some time ago a number of crystal structures have been reported for DPP and F_xDPP

systems.[5,9,52] These investigations have shown that all of the dodecaphenylporphyrins have very nonplanar structures compared to porphyrins without peripheral steric crowding, but have also revealed a higher degree of structurally heterogeneity (i.e. differences in the amount and type of distortion) in comparison to other classes of highly substituted nonplanar porphyrins.[9] Additional studies of the F_xDPPs may reveal what influence, if any, this structural heterogeneity has on the chemical, electrochemical, and spectroscopic properties of this unusual series of porphyrins.

Acknowledgments

This work was supported by the U.S. Department of Energy Contract DE-ACO4-94AL85000 (J.A.S.), the Robert A. Welch Foundation (E-680, K.M.K.), the National Science Foundation (CHE-96-23117) (K.M.S.), and by a Grant-in-Aid for Scientific Research Priority Areas (Nos. 10146232 and 10149230) from the Ministry of Education, Science, Culture and Sports of Japan (S.F.).

References

(1) Barkigia, K. M.; Berber, M. D.; Fajer, J.; Medforth, C. J.; Renner, M. W.; Smith, K. M. *J. Am. Chem. Soc.* **1990**, *112*, 8851.

(2) Barkigia, K. M.; Chantranupong, L.; Smith, K. M.; Fajer, J. *J. Am. Chem. Soc.* **1988**, *110*, 7566.

(3) Renner, M. W.; Barkigia, K. M.; Zhang, Y.; Medforth, C. J.; Smith, K. M.; Fajer, J. *J. Am. Chem. Soc.* **1994**, *116*, 8582.

(4) Sparks, L. D.; Medforth, C. J.; Park, M.-S.; Chamberlain, J. R.; Ondrias, M. R.; Senge, M. O.; Smith, K. M.; Shelnutt, J. A. *J. Am. Chem. Soc.* **1993**, *115*, 581.

(5) Barkigia, K. M.; Nurco, D. J.; Renner, M. W.; Melamed, D.; Smith, K. M.; Fajer, J. *J. Phys. Chem. B* **1998**, *102*, 322.

(6) Drain, C. M.; Kirmaier, C.; Medforth, C. J.; Nurco, D. J.; Smith, K. M.; Holten, D. *J. Phys. Chem. Soc.* **1996**, *100*, 11984.

(7) Gentemann, S.; Nelson, N. Y.; Jaquinod, L.; Nurco, D. J.; Leung, S. H.; Medforth, C. J.; Smith, K. M.; Fajer, J.; Holten, D. *J. Phys. Chem. B* **1997**, *101*, 1247.

(8) Medforth, C. J.; Smith, K. M. *Tetrahedron Lett.* **1990**, *31*, 5583.

(9) Nurco, D. J.; Medforth, C. J.; Forsyth, T. P.; Olmstead, M. M.; Smith, K. M. *J. Am. Chem. Soc.* **1996**, *118*, 10918.

(10) Hobbs, J. D.; Majumder, S. A.; Luo, L.; Sickelsmith, G. A.; Quirke, J. M. E.; Medforth, C. J.; Smith, K. M.; Shelnutt, J. A. *J. Am. Chem. Soc.* **1994**, *116*, 3261.

(11) Senge, M. O.; Smith, K. M. *J. Chem. Soc., Chem. Commun.* **1994**, 923.

(12) Bhyrappa, P.; Krishnan, V. *Inorg. Chem.* **1991**, *30*, 239.

(13) Bhyrappa, P.; Krishnan, V.; Nethaji, M. *J. Chem Soc., Dalton Trans.* **1993**, 1901.

(14) Bhyrappa, P.; Krishnan, V.; Nethaji, M. *Chem. Lett.* **1993**, 869.

(15) Wijesekera, T.; Matsumoto, A.; Dolphin, D.; Lexa, D. *Angew. Chem. Int. Ed. Engl.* **1990**, *29*, 1028.

(16) Shelnutt, J. A.; Song, X.-Z.; Jentzen, W.; Ma, J. G.; Medforth, C. J. *Chem. Soc. Rev.*

1998, *27*, 31.

(17) D'Souza, F.; Villard, A.; Caemelbecke, E. V.; Franzen, M.; Boschi, R.; Tagiagtesta, P.; Kadish, K. M. *Inorg. Chem.* **1993**, *32*, 4042.

(18) Kadish, K.; D'Souza, F.; Villard, A.; Autret, M.; Van Caemelbecke, E.; Bianco, P.; Antonini, A.; Tagliatesta, P. *Inorg. Chem.* **1994**, *33*, 5169.

(19) Tagliatesta, P.; Li, J.; Autret, M.; Van Caemelbecke, E.; Villard, A.; D'Souza, F.; Kadish, K. *Inorg. Chem.* **1996**, *35*, 5570.

(20) Kadish, K. M.; Li, J.; van Caemelbecke, E.; Ou, Z.; Guo, N.; Autret, M.; D'Souza, F.; Tagliatesta, P. *Inorg. Chem.* **1997**, *36*, 6292.

(21) Jentzen, W.; Hobbs, J. D.; Simpson, M. C.; Taylor, K. K.; Ema, T.; Nelson, N. Y.; Medforth, C. J.; Smith, K. M.; Veyrat, M.; Mazzanti, M.; Ramasseul, R.; Marchon, J.-C.; Takeuchi, T.; Goddard, I., W. A.; Shelnutt, J. A. *J. Am. Chem. Soc.* **1995**, *117*, 11085.

(22) Harris, R. K.; Mann, B. E. *NMR and the Periodic Table*; Academic Press: 1978, pp 99.

(23) Green, M. K.; Medforth, C. J.; Muzzi, C. M.; Nurco, D. J.; Shea, K. M.; Smith, K. M.; Shelnutt, J. A.; Lebrilla, C. B. *Eur. Mass. Spect.* **1998**,

(24) Lin, X. Q.; Kadish, K. M. *Anal. Chem.* **1985**, *57*, 1498.

(25) Ohya-Nisiguchi, H. *Bull. Chem. Soc. Jpn.* **1979**, *52*, 2064.

(26) Friedman, M. *J. Org. Chem.* **1965**, *30*, 859.

(27) Williamson, K. L. *Macroscale and Microscale Organic Experiments*; D. C. Heath and Co.: Lexington, Massachusetts, 1989, pp 534.

(28) Wilcox, C. F. J. *Experimental Organic Chemistry, A Small Scal Approach*; MacMillan Publishing Co.: New York, 1988, pp 427.

(29) Selman; Eastman **1960**, *14*, 221.

(30) Medforth, C. J.; Senge, M. O.; Smith, K. M.; Sparks, L. D.; Shelnutt, J. A. *J. Am. Chem. Soc.* **1992**, *114*, 9859.

(31) Fuhrop, J.-H.; Smith, K. M. In *Porphyrins and Metalloporphyrins*; K. M. Smith, Ed.; Elsevier: Amsterdam, 1975.

(32) Takeda, J.; Sato, M. *Inorg. Chem.* **1992**, *31*, 2877.

(33) Takeda, J.; Sato, M. *Chemical & Pharmaceutical Bulletin* **1994**, *42*, 1005.

(34) Langry, K. C. Ph. D. Thesis, University of California at Davis, 1982.

(35) Guilard, R.; Perie, K.; Barbe, J.-M.; Nurco, D.; Smith, K. M.; Van Caemelbecke, E.; Kadish, K. M. *Inorg. Chem.* **1998**, *37*, 973.

(36) Chamber, R. D.; Clark, M.; Spring, D. J. *J. Chem. Soc., Perkin Trans. 1* **1972**, 2464.

(37) Barton, D. H.; Zard, S. Z. *J. Chem. Soc., Chem. Commum* **1985**, 1098.

(38) Ono, N.; Maruyama, K. *Bull. Chem. Soc. Jpn.* **1988**, *61*, 4470.

(39) Kaesler, R. W.; LeGoff, E. *J. Org. Chem.* **1982**, *47*, 5246.

(40) Zhou, X.; Tse, M. K.; Wan, T. S.; Chan, K. S. *J. Org. Chem.* **1996**, *61*, 3590.

(41) Muzzi, C. M.; Ma, J.; Medforth, C. J.; Nurco, D. J.; Clement, T. E.; Khoury, R. G.; Smith, K. M.; Cancilla, M.; Voss, L.; Lebrilla, C.; Shelnutt, J. A. manuscript in preparation

(42) Kadish, K. M. *Prog. Inorg. Chem.* **1986**, *34*, 435.

(43) Kadish, K. M. In *Iron Porphyrins*; A. B. P. Lever and H. B. Gray, Ed.; Addison-Wesley: 1983; pp 161.

(44) Lexa, D.; Mispelter, J.; Saveant, J. M. *J. Am. Chem. Soc.* **1981**, *103*, 6806.

(45) Takeda, J.; Sato, M. *Chem. Lett.* **1995**, 939.

(46) Barkigia, K. M.; Renner, M. W.; Furenlid, L. R.; Medforth, C. J.; Smith, K. M.; Fajer, J. *J. Am. Chem. Soc.* **1993**, *115*, 3627.

(47) Kadish, K. M.; Van Caemelbecke, E.; D'Souza, F.; Lin, M.; Forsyth, T. P.; Medforth, C. J.; Krattinger, B.; Nurco, D. J.; Smith, K. M.; Shelnutt, J. A. manuscript in preparation

(48) Kadish, K. M.; Rhodes, R. K. *Inorg. Chem.* **1983**, *22*, 1090.

(49) Grinstaff, M. W.; Hill, M. G.; Labinger, J. A.; Gray, H. G. *Science* **1994**, *264*, 1311.

(50) Donohoe, R. J.; Atamian, M.; Bocian, D. F. *J. Am. Chem. Soc.* **1987**, *109*, 5593.

(51) Yamaguchi, K.; Morishima, I. *Inorg. Chem.* **1992**, *31*, 3216.

(52) Nurco, D. J. Ph. D. Thesis, University of California at Davis, 1998.

Table 1. Half-Wave Potentials ($E_{1/2}$, V vs. SCE) for Oxidation of Chloroiron(III) Porphyrins in CH_2Cl_2, 0.1 M TBAP.

Porphyrin	1st Ox	2nd Ox	Δ (Ox)
OEP[42,43]	1.08	1.30	0.22
TPP[42,43]	1.14	1.43	0.29
DPP	0.73	1.19	0.46
F_4DPP	0.78	1.16	0.38
F_8DPP (β)	0.82	1.19	0.37
F_{12}DPP	0.84	1.18	0.34
F_8DPP (meso)	1.06	1.41	0.35
F_{20}DPP	1.36	1.64	0.28
F_{28}DPP	1.45	[a]	---
F_{36}DPP	1.40[b]	[a]	---
$\Delta_{\text{FLUORINATION}}$[c]	+0.72	+0.45	

[a]Process occurs at potentials too positive to measure.

[b]E_{pa} at a scan rate of 0.1 V/s.

[c]Anodic shift for most highly fluorinated derivative versus least fluorinated derivative.

Table 2. Potentials (V vs. SCE) for Reduction of Chloroiron(III) Porphyrins in Benzonitrile Containing 0.1 M TBAP.

Porphyrin	1st Red			2nd Red			3rd Red
	E_{pc} (I')	E_{pa} (I)	Δ^a (V)	E_{pc} (II')	E_{pa} (II)	Δ^a (V)	$E_{1/2}$ (III)
OEP	-0.54[b]			-1.26[b]			
TPP	-0.29[b]			-1.06[b]			-1.73
DPP	-0.35[b]				-0.99[b]		-1.76
F_4DPP	-0.34	-0.01	0.33	-1.31	-0.90	0.41	-1.66
F_8DPP (β)	-0.33	0.01	0.34	-1.41	-0.87	0.54	-1.63
F_{12}DPP	-0.28	0.04	0.32	-1.24[c]	-0.84	0.40	-1.58
F_8DPP (meso)	-0.27	0.15	0.42	-1.42[d]	-0.91	0.51	-1.67
F_{20}DPP	-0.10	0.58	0.68	-1.14	-0.56	0.58	-1.37
F_{28}DPP	-0.04	0.47	0.51	-1.12	-0.46	0.66	-1.28
F_{36}DPP	+0.12	0.85	0.73	-0.88	-0.30	0.58	-1.10
$\Delta_{FLUORINATION}$[e]	+0.45	+0.86		+0.43	+0.69		+0.66

[a] $\Delta = |E_{pc} - E_{pa}|$

[b] $E_{1/2}$ value.

[c] Additional reversible reaction seen at -0.90 V.

[d] Additional peak potential at -1.18 V.

[e] Anodic shift for most highly fluorinated derivative versus least fluorinated derivative.

Table 3. Absorption Maxima for $FeF_{20}DPPCl$ and its Electroreduced Products in Benzonitrile and Pyridine Containing 0.2 M TBAP.

Redox Reaction	Solvent	λ_{max}, nm			
none	benzonitrile	389	432		
	pyridine	348	441		586
1st Red	benzonitrile	327	432	534	568
	pyridine	351	447	551	588
2nd Red	benzonitrile	319	422	605	738
	pyridine	323	430	609	794
3rd Red	benzonitrile	311	486	574	
	pyridine	310	475	568	736

Table 4. Half-Wave Potentials (V vs SCE) for Reduction of Chloroiron(III) Porphyrin Complexes in Pyridine Containing 0.1 M TBAP.

Porphyrin	1st Red Process I	2nd Red Process II	3rd Red Process III
OEP[42,43]	-0.02	-1.80	
TPP[42,43]	0.17	-1.45	
DPP	-0.01	-1.58	-1.85
F_4DPP	0.06	-1.50	-1.76
F_8DPP (β)	0.09	-1.48	-1.75
F_{12}DPP	0.07	-1.44	-1.74
F_8DPP (meso)	0.12	-1.49	-1.76
F_{20}DPP	0.45	-1.19	-1.53
F_{28}DPP	0.53	-1.07	-1.44
F_{36}DPP	0.58	-0.88	-1.27
$\Delta_{FLUORINATION}$[a]	0.59	0.70	0.58

[a]Anodic shift for most highly fluorinated derivative versus least fluorinated derivative.

Table 5. Half-wave Potentials (V vs. SCE) for Reductions of MDPP and $MF_{20}DPP$ Complexes[a] in Benzonitrile or CH_2Cl_2 with 0.1 M TBAP.

Porphyrin	Metal Ion	1st Red	2nd Red	Δ (V)
DPP	$Fe^{III}Cl$	-0.99	-1.76	0.77
	Zn	-1.34[45]	-1.70[45,b]	0.36
	Ni	-1.24	-1.72	0.48
	Cu	-1.22	-1.61	0.39
$F_{20}DPP$	$Fe^{III}Cl$	-1.14[b]	-1.37	0.23
	Zn	-1.04	-1.43	0.39
	Ni	-0.96	-1.45	0.49

[a]Details of the syntheses of the other metal complexes are given elsewhere.[52]

[b]E_{pc} for irreversible process.

Figure Captions.

Figure 1 Structures of the porphyrins discussed in this work.

Figure 2 Cyclic voltammograms for the electrooxidation of chloroiron(III) porphyrins in CH_2Cl_2/0.1 M TBAP. Scan rate = 0.1 V/s.

Figure 3 Cyclic voltammograms for electroreduction of the FeF_xDPPCl complexes in benzonitrile/0.1 M TBAP. Scan rate = 0.1 V/s.

Figure 4 Cyclic voltammograms for reduction of $FeF_{20}DPPCl$ in benzonitrile/0.1 M TBAP with and without excess TBACl. Scan rate = 0.1 V/s.

Figure 5 Spectral changes for the first, second and third one-electron reductions of $FeF_{20}DPPCl$ in (a) benzonitrile/0.2 M TBAP and (b) pyridine/0.2 M TBAP.

Figure 6 ESR spectra of doubly reduced $FeF_{20}DPPCl$ at 77 K in (a) benzonitrile/0.2 M TBAP and (b) pyridine/0.2 M TBAP. The spectra were generated *in-situ* after chemical reduction of the porphyrin using 2 equivalents of $Ru(bpy)_3^+$.

Figure 7 Cyclic voltammograms for electroreduction of the FeF_xDPPCl complexes in pyridine/0.1 M TBAP. Scan rate = 0.1 V/s.

Figure 8 Cyclic voltammograms of (a) MDPPs in benzonitrile/0.1 M TBAP, (b) $MF_{20}DPPs$ in benzonitrile/0.1 M TBAP or CH_2Cl_2/0.1 M TBAP, and (c) $MF_{20}DPPs$ in pyridine/0.1 M TBAP. M = Zn, Fe, Cu or Ni.

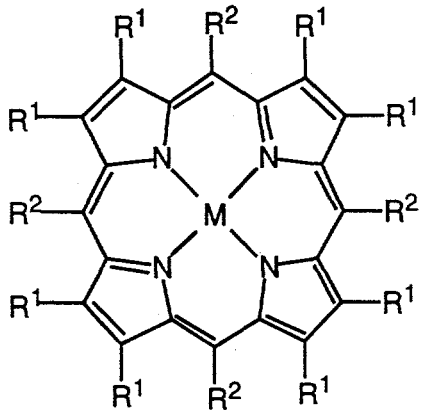

	R1	R2	M	Abbreviation
1	ethyl	phenyl	2H	
2	ethyl	NO_2	2H	
3	Br	phenyl	2H	
4	phenyl	phenyl	2H	
5	H	phenyl	$Fe^{III}Cl/Co^{II}$	
6	Br	phenyl	$Fe^{III}Cl/Co^{II}$	
7	H	methyl	Ni^{II}	
8	H	ethyl	Ni^{II}	
9	H	i-propyl	Ni^{II}	
10	H	t-butyl	Ni^{II}	
11	phenyl	4-fluorophenyl	2H	H_2F_4DPP
12	4-fluorophenyl	phenyl	2H	H_2F_8DPP (β)
13	phenyl	2,6-difluorophenyl	2H	H_2F_8DPP (meso)
14	4-fluorophenyl	4-fluorophenyl	2H	$H_2F_{12}DPP$
15	phenyl	pentafluorophenyl	2H	$H_2F_{20}DPP$
16	4-fluorophenyl	pentafluorophenyl	2H	$H_2F_{28}DPP$
17	3,5-difluorophenyl	pentafluorophenyl	2H	$H_2F_{36}DPP$
18	2,6-difluorophenyl	pentafluorophenyl	2H	$H_2F_{36}DPP$
19	pentafluorophenyl	pentafluorophenyl	2H	$H_2F_{60}DPP$
20	2,6-difluorophenyl	phenyl	2H	$H_2F_{16}DPP$
21	pentafluorophenyl	phenyl	2H	$H_2F_{40}DPP$

Figure 1

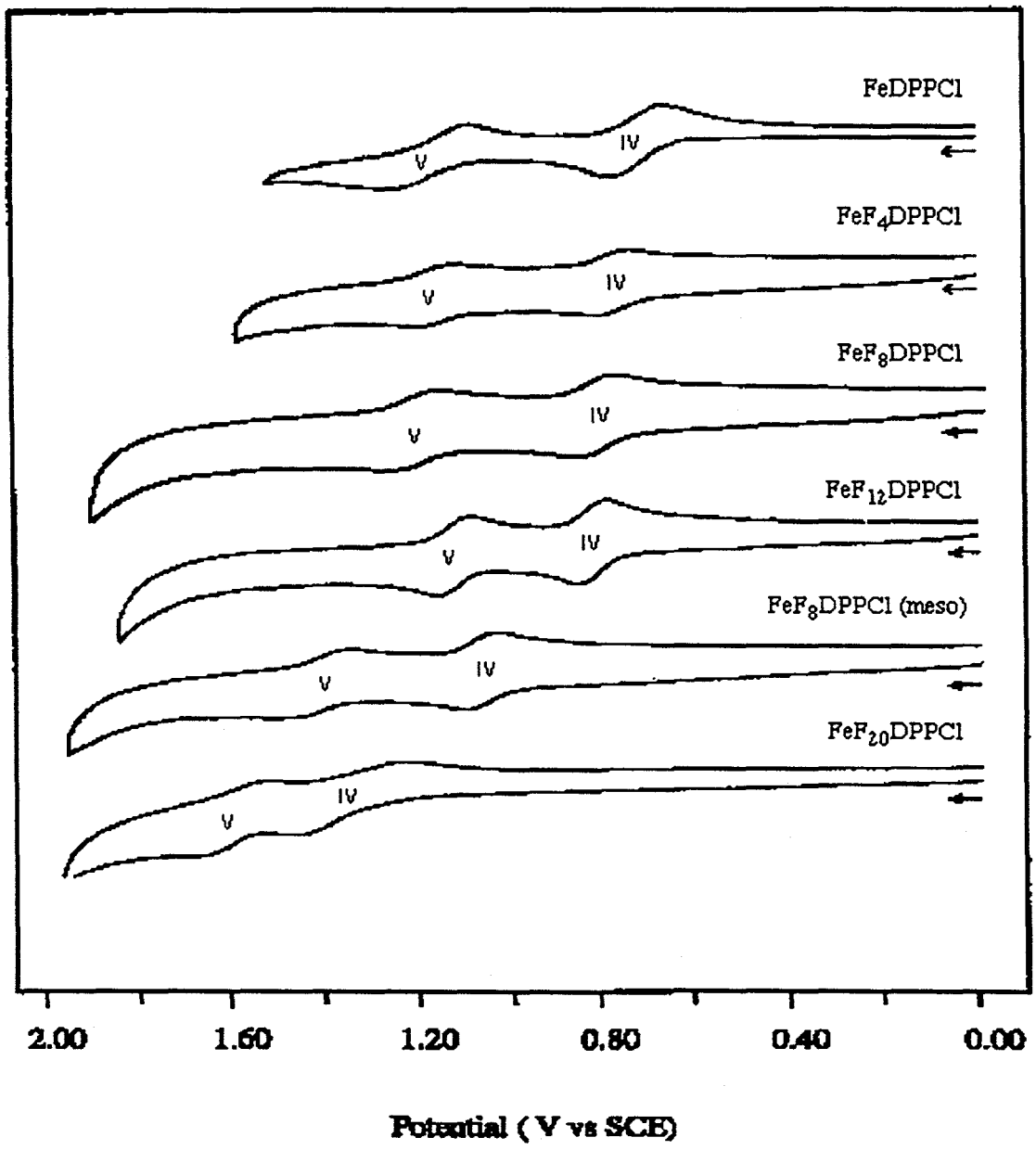
FeDPPCl
V
IV
FeF4DPPCl
V
IV
FeF8DPPCl
V
IV
FeF12DPPCl
V
IV
FeF8DPPCl (meso)
V
IV
FeF20DPPCl
V
IV
2.00
1.60
1.20
0.80
0.40
0.00
Potential (V vs SCE)

Figure 2.

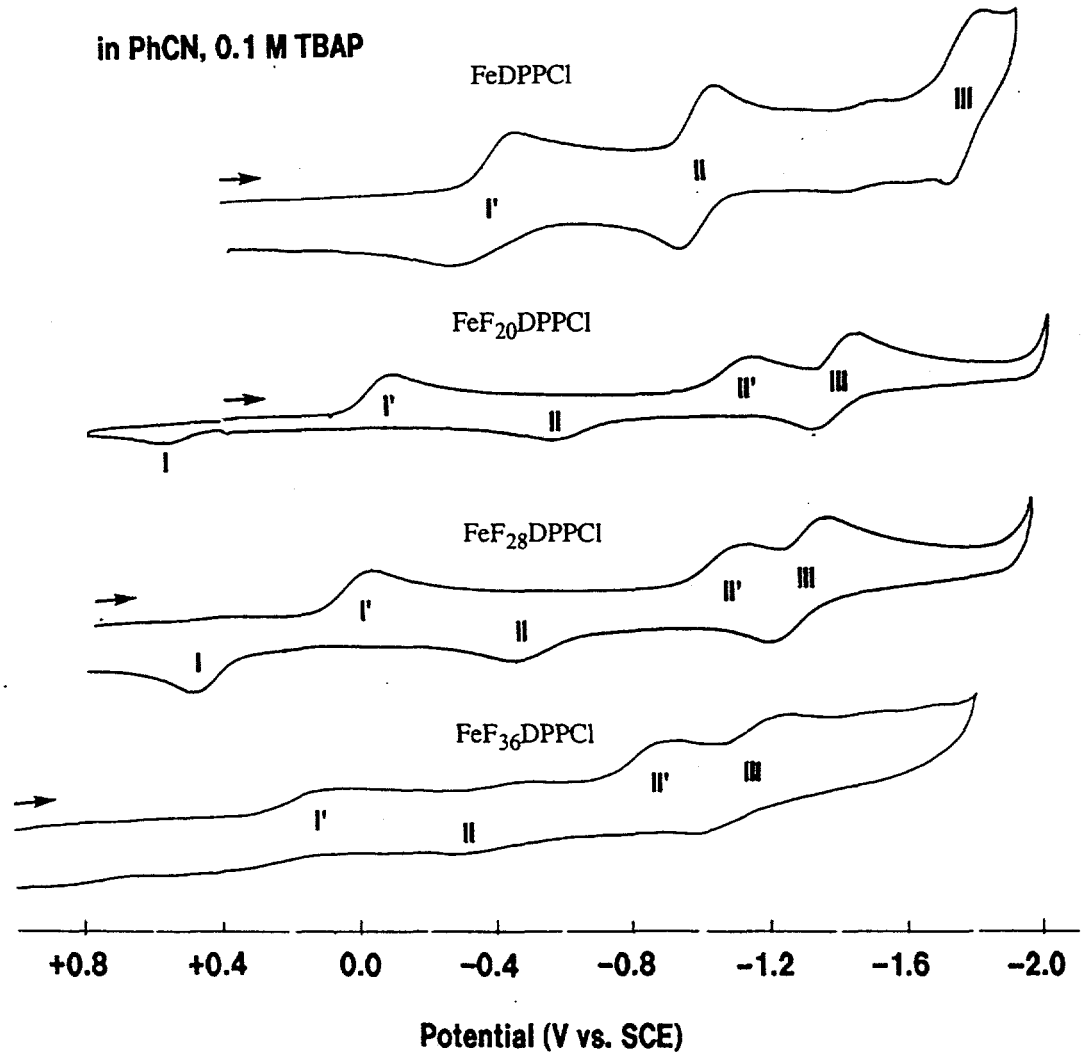

Figure 7

Figure 3.

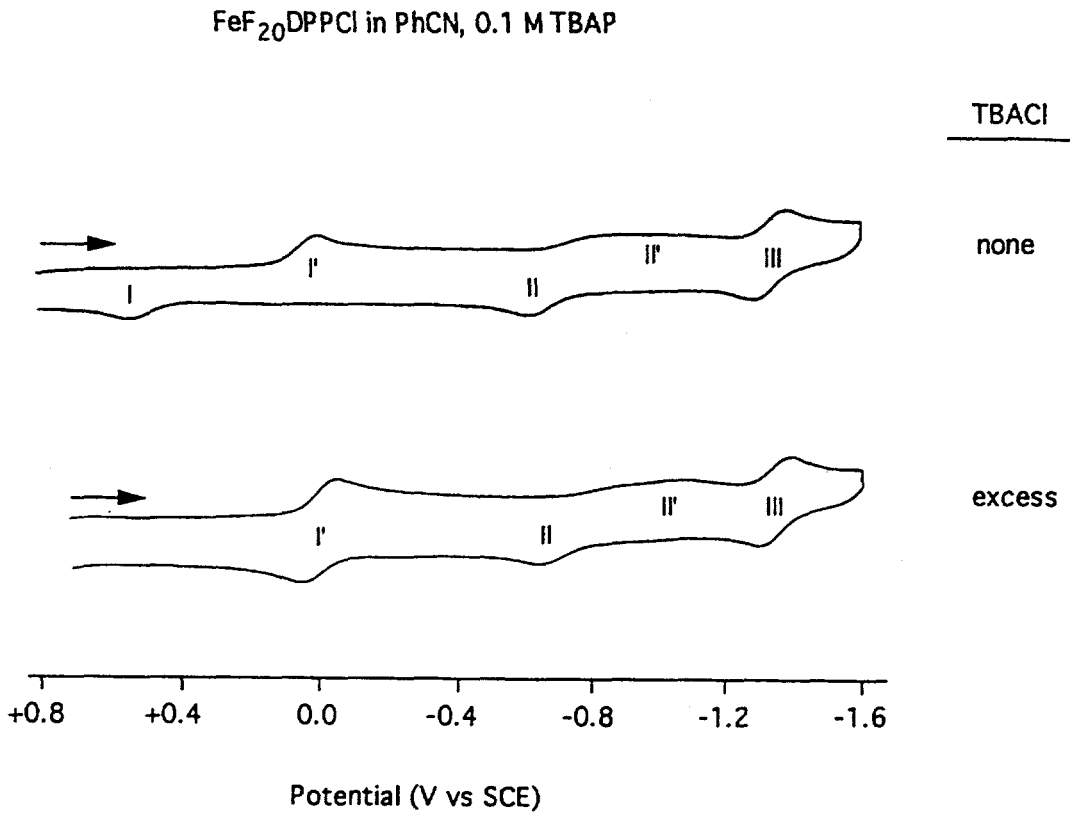
FeF20DPPCl in PhCN, 0.1 M TBAP
TBACl
none
excess
I
I'
II
II'
III
+0.8
+0.4
0.0
-0.4
-0.8
-1.2
-1.6
Potential (V vs SCE)

Figure 4.

$FeF_{20}DPPCl$

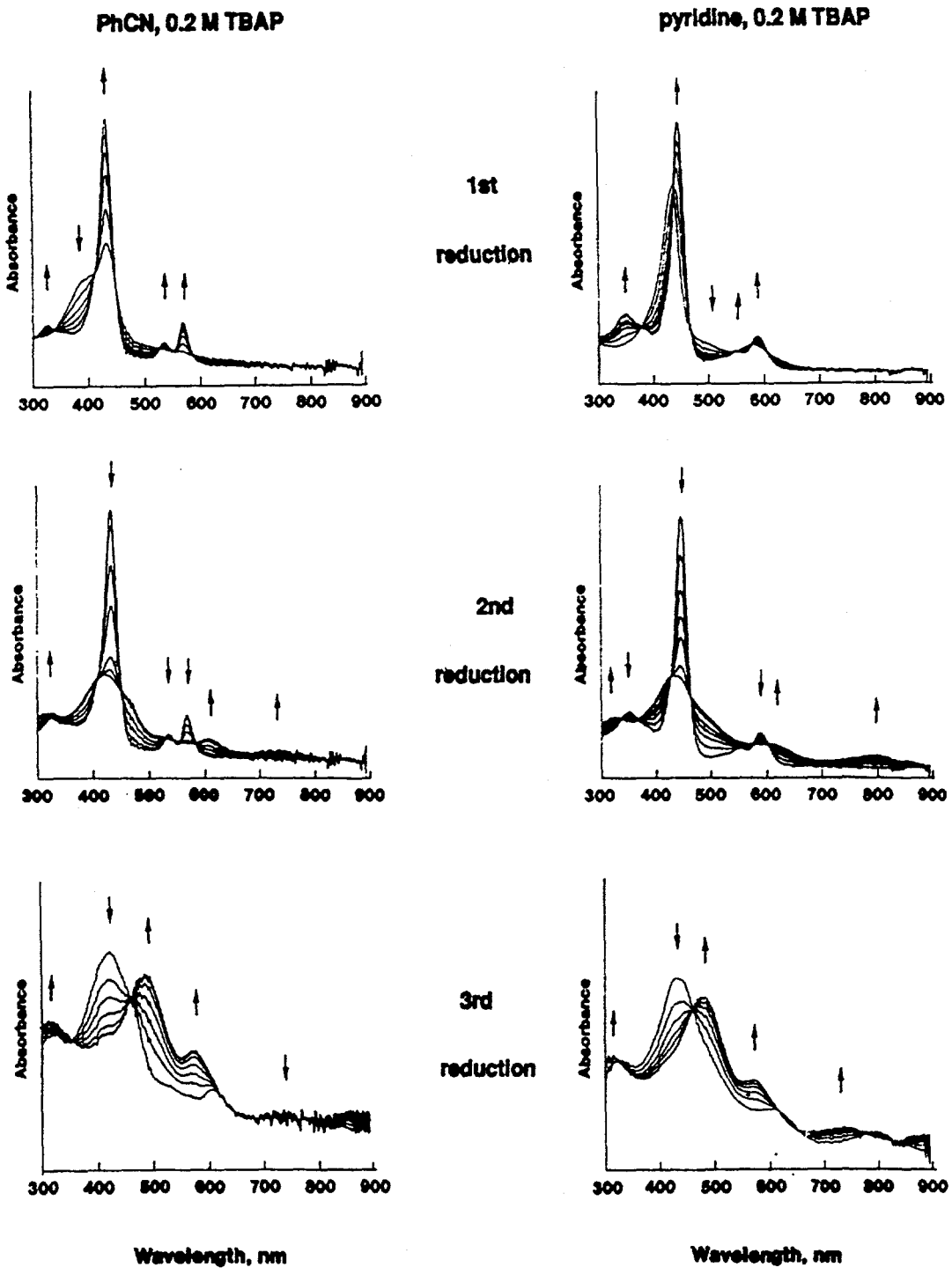

Figure 5.

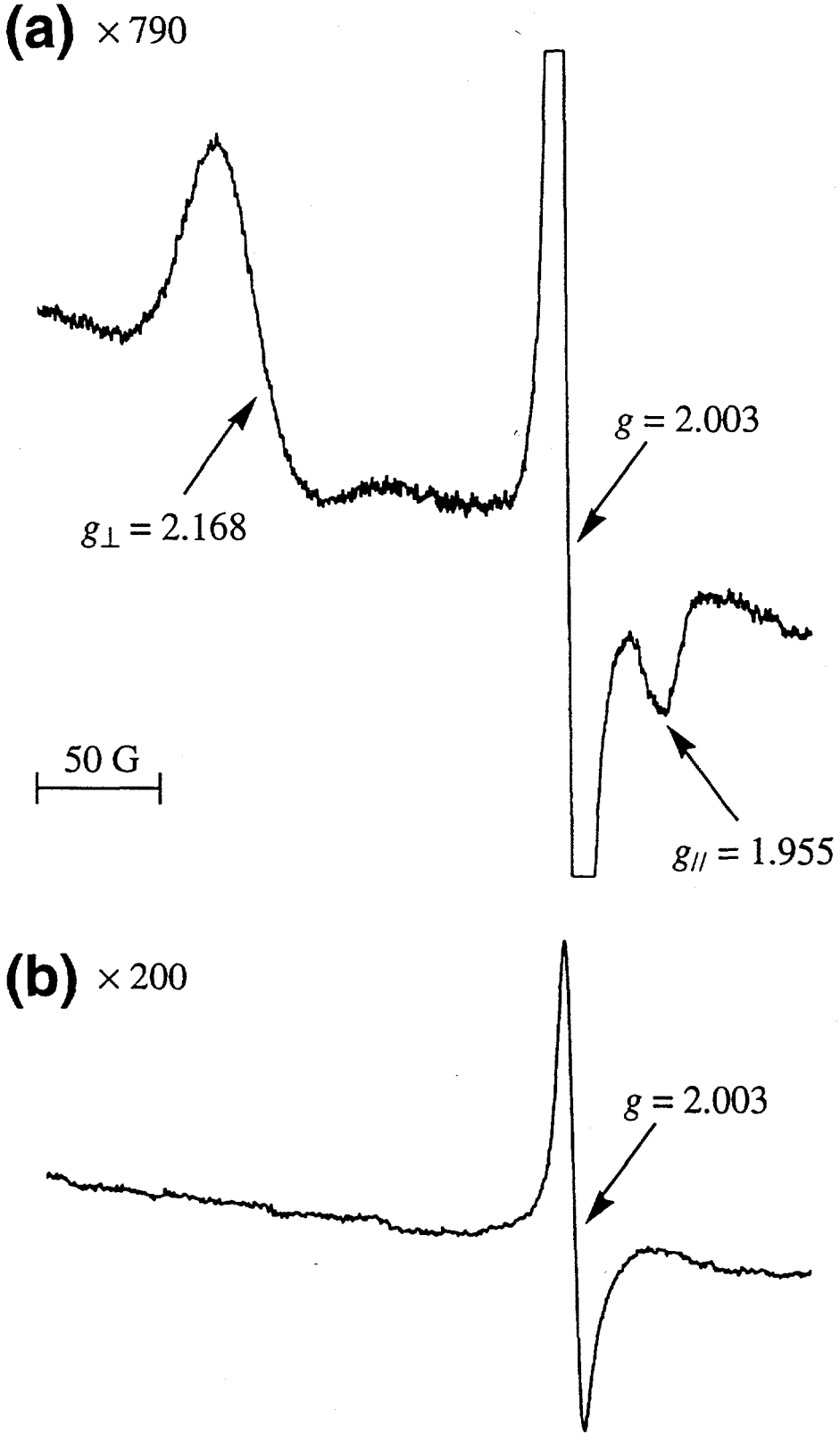

Figure 6.

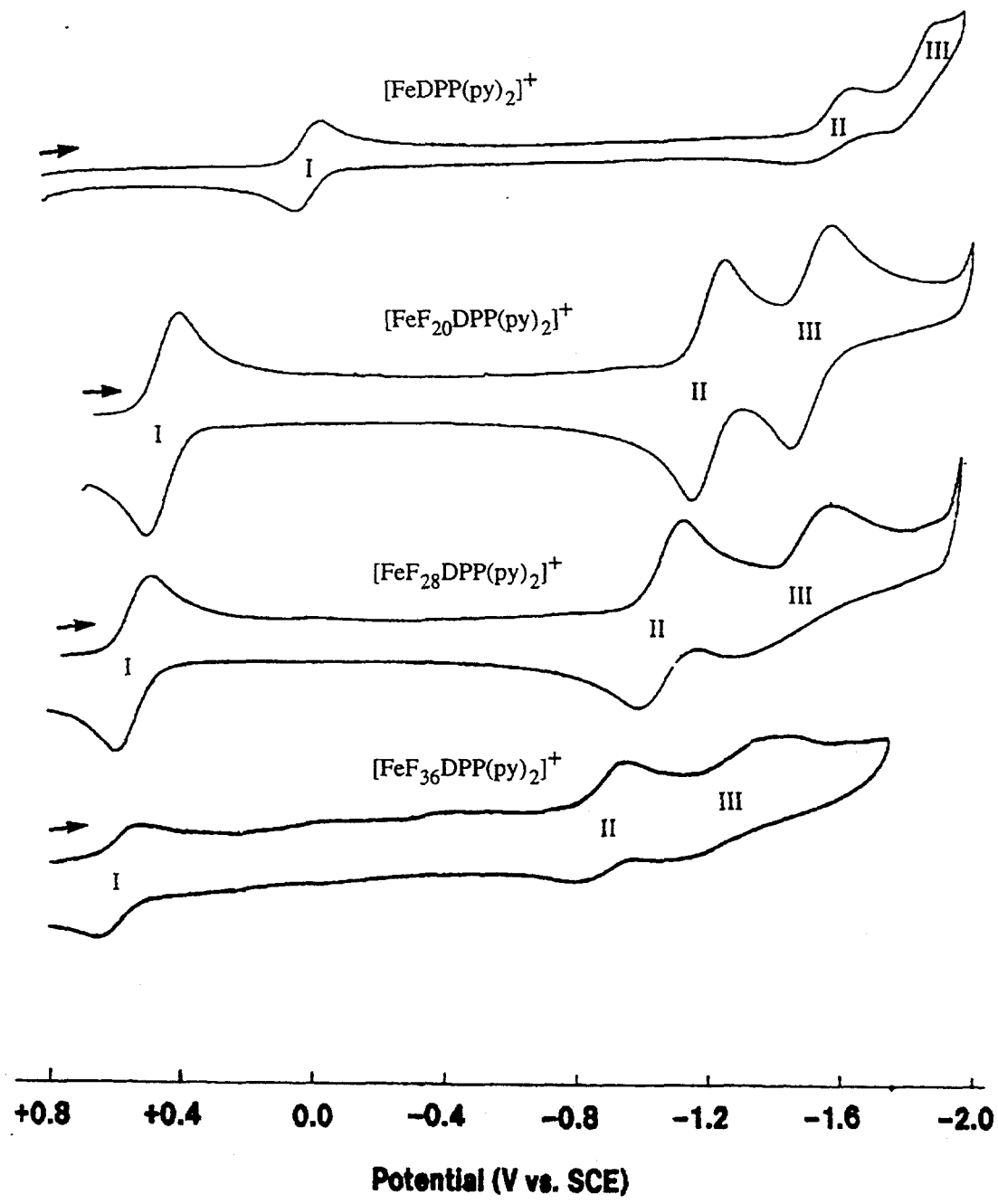

Figure 11

Figure 7.

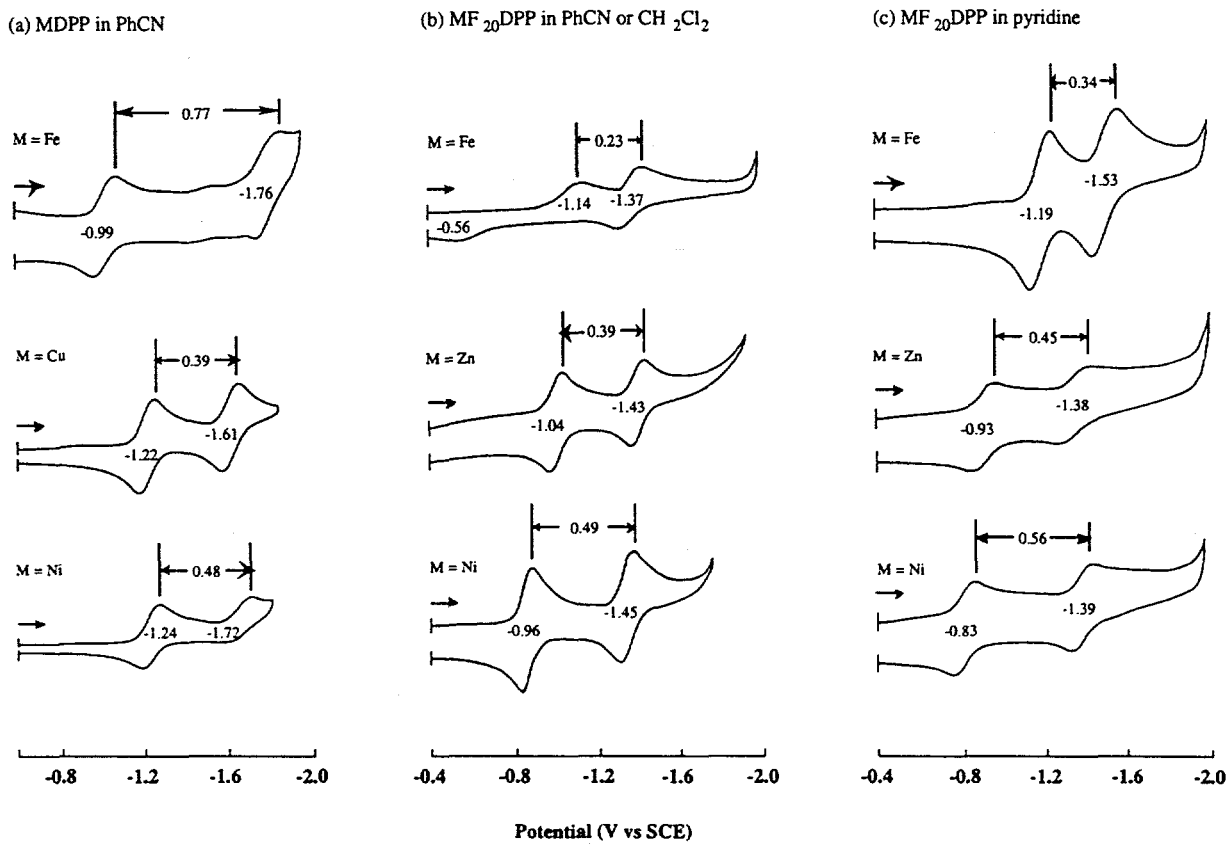
(a) MDPP in PhCN
(b) MF 20DPP in PhCN or CH 2Cl2
(c) MF 20DPP in pyridine
M = Fe
0.77
-1.76
-0.99
M = Cu
0.39
-1.61
-1.22
M = Ni
0.48
-1.24
-1.72
M = Fe
0.23
-1.14
-1.37
-0.56
M = Zn
0.39
-1.43
-1.04
M = Ni
0.49
-1.45
-0.96
M = Fe
0.34
-1.53
-1.19
M = Zn
0.45
-1.38
-0.93
M = Ni
0.56
-1.39
-0.83
-0.8 -1.2 -1.6 -2.0
-0.4 -0.8 -1.2 -1.6 -2.0
-0.4 -0.8 -1.2 -1.6 -2.0
Potential (V vs SCE)

Figure 8.